NTNU
Norwegian University of
Science and Technology

Preparation and surface modifications on hollow silica nano spheres

Nano- insulation

Per Solibakke

Chemical Engineering and Biotechnology
Submission date: July 2018
Supervisor: Mari-Ann Einarsrud, IMA
Co-supervisor: Malin Sletnes, SINTEF

Norwegian University of Science and Technology
Department of Materials Science and Engineering

Preparation and surface modifications on hollow silica nano-spheres

A future nano insulation material

Master thesis

by

Per Solibakke

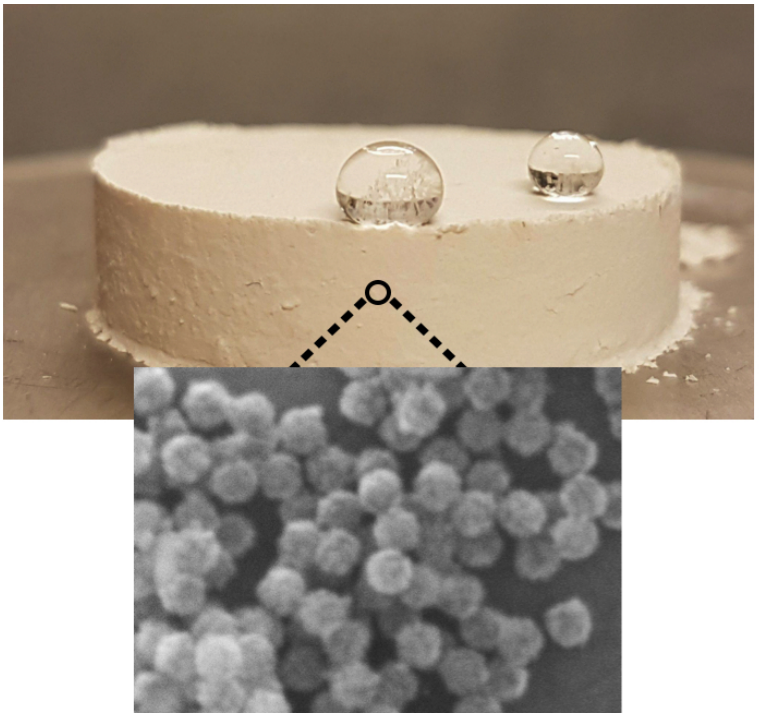

Declaration

I hereby declare that the work presented in this thesis has been preformed independently and in accordance with the rules and regulations of the Norwegian University of Science and Technology (NTNU).

Date: 06.07.2018

Per Solibakke

Preface

This thesis is submitted to the Norwegian University of Science and Technology (NTNU), as part of the requirements for the Master of Science. The work presented in this thesis has been carried out at the Department of Materials Science and Engineering at NTNU between 21 January and 6 July, 2018. Professor Mari - Ann Einarsrud has supervised the work, and Research Scientist Malin Sletnes has served as co - supervisor.

I would like to thank my supervisors for the time and effort they have laid down providing me with motivation and expertise during this work. Both my main supervisor Mari - Ann Einarsrud and my co - supervisor Malin Sletnes have provided exceptional detailed feedback during these six months, which has been especially helpful due to my dyslexia. My main supervisor Mari - Ann Einarsrud has provided me with an largely enhanced understanding of inorganic chemistry, along with solutions and constructive feedback which is reflected by the achieved results. My co - supervisor Malin Sletnes has provided me with exceptional knowledge concerning insulation both in a research perspective and a commercial perspective, along with innovating ideas and expertise in regards to preparation and modification of hollow silica nano spheres.

I would also like to acknowledge the people associated with the Functional Materials and Materials Chemistry group in general. Special credit goes to Researcher Tao Gao for giving me a introduction in hot disk thermal conductivity measurements along with his speciality within nano - insulation. Finally, I would like to thank all technical staff at the department, for giving me equipment training and assistance for any problems during my work.

Abstract

Hollow silica nano spheres (HSNS) were synthesised with the use of polystyrene templates. Based on the polystyrene templates, tetraethyl orthosilicate (TEOS) was hydrolysed and attached on the surface, in either an acidic or basic environment. The acidic catalyst, HCl and the basic catalyst, NH_4OH were investigated to determine the reaction yield and morphology generation. By repetitive experiments a hypothesis was developed. The morphology outcome is valid for an ammonia solution with a m% of NH_3 between 10 % to 30 %. The morphology of the attached silica and agglomeration of spheres were determined not to correspond directly with the pH, but rather the addition of ammonia solution. Moreover, the as - synthesised HSNS were modified by three separate surface modifications, to increase the hydrophobicity and reduce the brittleness. A hydroxylation process was necessary to re - attach hydroxide molecules, removed during heat treatment, for further modification. The hydroxylated HSNS exhibited moderate re - attachment of hydroxide molecules in basic water, providing that the required surface conditions. To increase the hydrophobicity a hydrophobisation process was attempted. HSNS were submerged in 20 % to 30 % hexamethyldisiloxane (HMDS), to attach large organic molecules on to the silica surface. The surface modification did not alter the hydrophobicity, nor did it effect the composition and morphology of the as - synthesised HSNS samples. To reduce the brittleness, a functionalisation process was developed. Vinyltrimethoxysilane (VMOS) was investigated, to analyse what effects, the attachment of $C = C$ bonds with large organic molecules on the silica surface, had on the hydrophobicity and thermal conductivity. For all functionalised HSNS, successful attachment of $C = C$ bonds was confirmed, along with a drastic transformation of hydrophobicity. A super hydrophobic material was created, with respect to a contact angle (θ) > 150 ° measured for all functionalised HSNS samples. The attachment of organic molecules and $C = C$ bonds did not alter the thermal conductivity and the $C = C$ bonds provides possibilities for continued modification of the material, reducing the brittleness.

The as - synthesised and surface modified HSNS were characterised with respect to their morphology (SEM) and composition (FTIR). The functionalised HSNS, along with their corresponding hydroxylated precursor, were characterised with respect to their hydrophobicity (contact angle). Selected as - synthesised and functionalised HSNS were characterised with respect to their thermal conductivity (Hot disk).

Sammendrag

Hule silika nano sfærer (HSNS) har blitt syntetisert ved bruk av polystyren templater. Basert på disse polystyren templatene, ble tetraethyl orthosilicate (TEOS) hydrolysert og tilkoblet til overflaten, i enten et surt eller basisk miljø. Syre katalysatoren HCl og base katalysatoren NH_4OH har blitt undersøkt for å avgjøre reaksjonsutbyttet og morfologien av sfærene og silika nano - partiklene. Ved gjentatte eksperiment har en hypotese blitt utviklet, angående struktur generasjonen. Hypotesen som ble utformet er gyldig med en m% av NH_3 mellom 10 % til 30 % i en ammoniakk løsning. Morfologien til de tilkoblede silika nano - partiklene og aggregering av sfærene var ikke direkte knyttet til pH, men heller mengden ammoniakk - løsning tilsatt. I tillegg ble de syntetiserte HSNS modifisert av tre ulike overflate modifikasjoner, for å øke hydrofobisiteten og redusere skjørheten til materialet. En hydroksylerings prosess var nødvendig for å koble hydroksyl grupper til silika overflaten, basert på forbrenningen av disse molekylene under varmebehandlingen. De hydroksylerte HSNS erfarte en moderat tilknytning av hydroksyl grupper i basisk vann og genererte den nødvendige overflate strukturen for videre modifikasjoner. For øking av hydrofobisiteten ble en hydrofobiserings prosess forsøkt. Hydroksylerte HSNS ble integrert i en løsning av 20 % - 30 % hexamethoxysilane (HMDS), for å tilkoble store organiske molekyler på silika overflaten. Overflate modifikasjonen forandret ikke hydrofobisiteten, morfologien eller komposisjonen til hydroksylerte HSNS. For å redusere skjørheten, ble en funksjonaliserings prosess utviklet. Kjemikalet vinyltrimethoxysilane (VMOS) ble undersøkt, for å analysere hvordan tilkoblingen av $C = C$ bindinger med store organiske grupper på silika overflaten, påvirket den termiske konduktiviteten og hydrofobisiteten. Alle funksjonaliserte HSNS materialer hadde en suksessfull tilkobling av $C = C$ bindinger og i tillegg en drastisk forandring i hydrofobisitet. Et super hydrofobt material ble laget, i tilknytning til en kontakt vinkelen (θ) > 150 °, målt for alle funksjonaliserte HSNS materialer. Tilkoblingen av organiske grupper samt $C = C$ bindinger, påvirket ikke den termiske konduktiviteten og $C = C$ bindingene genererer muligheter for videre modifikasjon og dermed redusere skjørheten til materialet.

Syntetiserte og overflate modifiserte HSNS ble karakterisert basert på deres morfologi (SEM) og komposisjon (FTIR). De funksjonaliserte HSNS, sammen med deres respektive forløpere, ble karakterisert basert på deres hydrofobisitet (kontakt vinkel). Valgte syntetiserte og funksjonaliserte HSNS ble karakterisert basert på deres termiske konduktivitet.

Contents

Chapter 1

Introduction

1.1 Motivation

The earliest accounts for employing insulation was done by the ancient Egypt (3000 BC), constructing buildings out of mud bricks for their ability to keep cool. The ancient greeks (900 BC - 600 AD) provided the next advancement integrating asbestos in fabrics and buildings based on their "mythical powers" concerning fire resistance. Further advances did not arrive before after the industrial revolution when Games Slayter invented a method for production of glass wool (a type of mineral wool) in 1933 [1]. Asbestos was at a large scale used until 1990s before it was banned in most western countries due to its health hazards [2]. The late ban is considered ironic since the ancient greeks noticed and documented the health effects it had on workers [3]. Games Slayter's glass wool and other types of mineral wool are the most employed insulation material today. However, research the last three decades has developed new materials with an extremely low heat conduction. Some of these super insulation materials (SIM) have already been used in applications requiring an extremely low thermal conductivity. These materials are normally only used for special applications, requiring high thermal insulation in a restricted space, due to high costs and durability issues.

In the EU, based on statistics from Eurostat in 2016, 65 % [4] of the energy consumption in residential sector goes towards space heating (Figure 1.1). Employing insulation materials with an extremely low thermal conductivity com-

pared to conventional insulation materials would not only reduce the energy requirements, but also reduce the space required of the insulation materials.

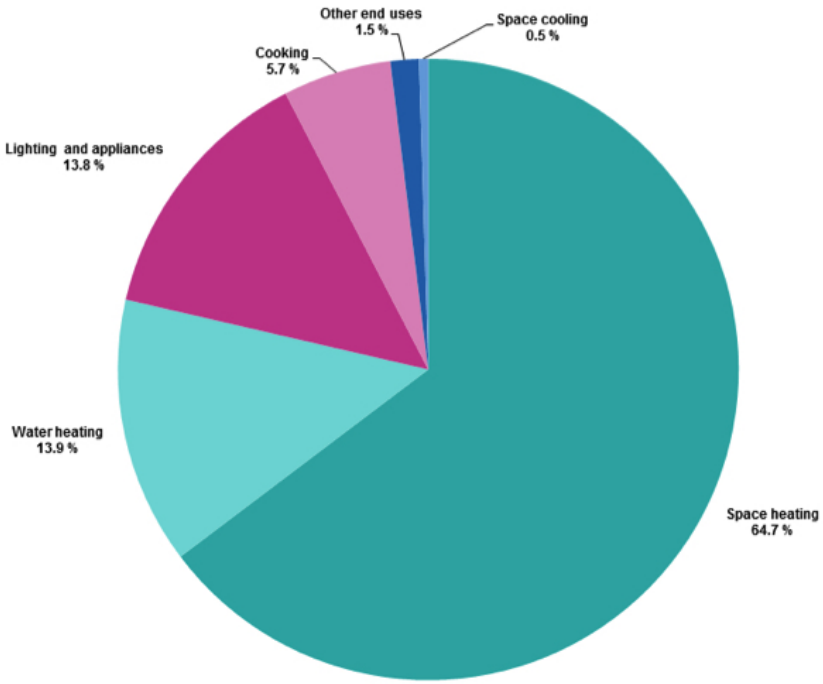

Figure 1.1: Pie-chart illustrating the energy consumption in the residential sector in Europe 2016 based in the statistical data from Eurostat[4].

A promising nano material, exhibiting a very low thermal conductivity has been under the microscope for the last 10 years. This nano - material, hollow silica nano spheres (HSNS) when synthesised, exhibits properties not suitable for insulation proposes. Adsorption of water and brittleness are the two key disadvantages. Modifying these properties, would produce a nano - insulation material that can revolutionise insulation used in the residential sector.

1.2 Aim of the work

The aim of this Master's thesis was to synthesise hollow silica nano-spheres (HSNS) for deployment in thermal insulation. Furthermore the surface of hollow silica nano-spheres should be modified to provide hydrophobic properties along with a less brittle structure more suitable for insulation applications. The synthesised HSNS should be characterised with respect to their morphology, size, chemical composition, hydrophobicity and thermal conductivity. The surface modified HSNS should be characterised with respect to their composition, hydrophobicity and thermal conductivity compared to their as - synthesised precursor.

Chapter 2

Background

2.1 Thermal conductivity

Thermal conduction

Particle collisions and electron movement are the main contributors to thermal conduction. Above absolute zero (-273.15 $^{\circ}C$) molecules/atoms vibrate depending on internal energy. At elevated temperatures these particles would have a rapid vibration, increasing the amounts of collisions per unit time. Each collision results in a transfer of kinetic and potential energy generating a flow of heat between the particles. Figure 2.1 illustrates a material effected by an external source of energy at one part of the surface. The microscopic particles closest, quickly increase their internal energy. The enhanced internal energy promotes a rapid vibration, increasing the amount of collisions with neighbouring particles. These collisions transfer the newly acquired internal energy in terms of kinetic and potential energy from the closest particles to particles further away from the heat source. In other words a flow of heat is generated throughout the material. The thermal conductivity of a material is highly dependent on its density. Generally solids conduct heat better than liquids and gases with respect to their closely packed structure of atoms. Atoms with small distances between each other have a larger possibility of colliding, transferring kinetic and potential energy at a higher magnitude. The freedom of movement of electrons also promotes thermal conductance. Metallic bonds consisting of a "sea" of electrons has a large degree of freedom and can move with relative ease throughout the material, while covalent and ionic bonds promote localised electrons [5].

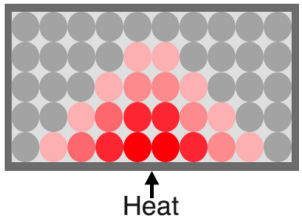

Figure 2.1: Illustration of heat propagation throughout a material affected by an external source of energy.

Figure 2.2 illustrates the general density difference between solids (a), liquids (b) and gases (c). Assuming identical conditions, the molecules exhibit a similar vibration. Hence the amount of collisions and movements of electrons between particles would be large for solids compared to gases with respect to the large volumetric space each molecule/atom in a gas can occupy.

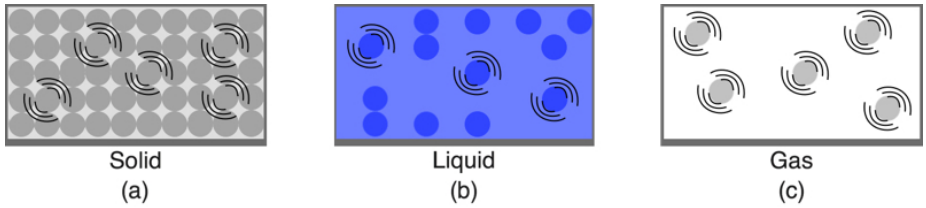

Figure 2.2: Illustration of structural differences between solids (a), liquids (b) and gases (c).

Generally the thermal conductivity (κ) of a material is treated as a constant, changing only based on the temperature. Still in many materials the thermal conductivity is relatively unchanged over a significant temperature range. The structure throughout the materials also affects the thermal conductivity. E.g. a non-uniform material would have variations in thermal conductivity at spatial locations while an anisotropic material has a variation of thermal conductivity based on orientation.

Law of heat conduction

Fourier's law, also known as the law of heat conduction, describes the rate of heat transfer [6]. The differential form (Equation 2.1), describes flow rates of energy locally based on fluxes, while the integration form (Equation 2.2), describes the complete flow of energy in and out of an object.

$$\overrightarrow{q} = -\kappa \nabla T \tag{2.1}$$

Where $\overrightarrow{q}$ is the local heat flux density $[Wm^{-2}]$, κ is the thermal conductivity of the material $[Wm^{-1}K^{-1}]$, treated as a constant and ∇T is the temperature gradient $[Km^{-1}]$.

By integrating the differential form (Equation 2.1) over the total surface area of the object, the integration form of Fourier's law is achieved.

$$\frac{\delta Q}{\delta t} = -\kappa \oiint_S \nabla T \times dS \tag{2.2}$$

Where Q is the overall heat $[W]$, $\frac{\delta Q}{\delta t}$ is the heat transferred per unit time $[Ws^{-1}]$ and dS is the surface area $[m^2]$.

For many applications a one-dimensional form of Fourier's law is sufficient treating both the differential Equation (2.1) and the integration equation (2.2) in only the x-direction.

$$q_x = -\kappa \frac{dT}{dx} \tag{2.3}$$

Where $\frac{dT}{dx}$ is the temperature difference in x-direction.

The one - dimensional integration form of Fourier's law is derived by integrating the one - dimensional differential Equation (2.3) over a homogenous material with a constant temperature.

$$\frac{Q}{\Delta t} = -\kappa A \times \frac{\Delta T}{\Delta x} \tag{2.4}$$

Where ΔT is the temperature difference between x_{start} and x_{end}, Δx is the distance between x_{start} and x_{end} and A is the surface area of the object.

A common term describing heat transfer in a material or a binding element with a specific thickness in one - dimension is the thermal conductance U, defined as the thermal conductivity (κ) of the material divided by the thickness (Δx) of the material:

$$U = \frac{\kappa}{\Delta x} \tag{2.5}$$

Adjusting the one - dimensional integration Equation (2.4) of Fourier's law to:

$$\frac{Q}{\Delta t} = -UA \times \Delta T \tag{2.6}$$

Thermal conductance (U) describes how effective a material transfers heat, thermal resistance (R) , the reciprocal, describes how a material resists heat flow.

$$R = \frac{1}{U} = \frac{\kappa}{\Delta x} \tag{2.7}$$

Where R is the thermal resistance ($m^2 K W^{-1}$).

For many applications especially in the building sector a high resistance towards heat flow is required. In most cases an object would consist of more than one layer of materials, each exhibiting an individual thermal conductance (U). The total thermal resistance (R_T) can be defined as the addition of individual thermal resistances (Equation (2.8)) or the addition of the reverse individual thermal conductances (Equation (2.9)).

$$R_T = R_1 + R_2 + ... + R_n \tag{2.8}$$

$$R_T = \frac{1}{U_1} + \frac{1}{U_2} + ... + \frac{1}{U_n} \tag{2.9}$$

Where n is the amount of layers in the object.

Both Equations 2.8 and 2.9 are based on the assumption that the energy moves as a straight line, perpendicular to each layer and that the energy is not diverted when in contact with a new material.

2.2 Thermal insulation

Insulating materials

Insulating materials exhibit a thermal conductivity below 0.065 $[Wm^{-1}K^{-1}]$ at regular conditions [7]. Table 2.1 lists common construction materials for different applications and their thermal conductivities.

Aluminium and iron are classic examples of metals with a closely packed structure and metallic bonds, promoting a large thermal conductivity. These materials are essential to construct objects exhibiting the required mechanical strength. E.g. aluminium produces light and mechanical strong objects.
Mineral wool and expanded polystyrene (EPS) exhibit a thermal conductivity below 0.065 $[Wm^{-1}K^{-1}]$ and are by definition insulating materials. These materials lack the mechanical strength compared to aluminium and iron. However, these materials are currently, the most used insulation materials and called conventional insulation in most sectors.

Table 2.1: Thermal conductivity's of different materials commonly used for construction [8].

Material	κ $[Wm^{-1}K^{-1}]$
Aluminum	210
Iron	80.5
Wood	0.21
Mineral wool	0.035
EPS	0.035

Insulation in wet conditions

In wet conditions, insulation materials are effected by water. The materials exhibit either hydrophobic (e.g EPS) or hydrophilic (e.g Sheepswool) properties. A hydrophobic insulation material does not adsorb water and would generate droplets on the surface in case of condensation. A hydrophilic material either

adsorbs water or forms a film of water on the surface. For hydrophilic materials, water adsorbed or deposited on the surface has the potential to be released once the humidity levels drops [9].

Constructions

Generally the construction pattern concerning walls in buildings consist of combining different layers of materials. The construction process should produce a wall both mechanically strong and with a low rate of heat flow. The heat flow through a wall is described by the total thermal conductance (U_T), also called the $U-value$ [10] and is the reverse of the total thermal resistance (R_T) (Equation 2.8 and 2.9).

Figure 2.3 illustrates a wall consisting of different layers of materials, each with different thickness and thermal conductivity. Based on the definition of U, Equation(2.5) and utilising Equation (2.9), a mathematical description for the total thermal resistance of the wall (R_T^{Wall}) can be estimated.

$$R_T^{Wall} = \frac{1}{U_{OS}} + \frac{L_1}{\kappa_{Wood}} + \frac{L_2}{\kappa_{MW}} + \frac{L_3}{\kappa_{Air}} + \frac{1}{U_{IS}} \tag{2.10}$$

Where U_{OS} and U_{IS} are the thermal conductance for the outer surface and the inner surface, κ_{Wood}, κ_{MW} and κ_{Air} is the thermal conductivity for wood, mineral wool and air and L_1, L_2 and L_3 is the thickness of wood, mineral wool and air, respectively.

The $U-value$ of the wall can then be expressed as the reverse of the total thermal resistance:

$$U - value = \frac{1}{R_T^{Wall}} \tag{2.11}$$

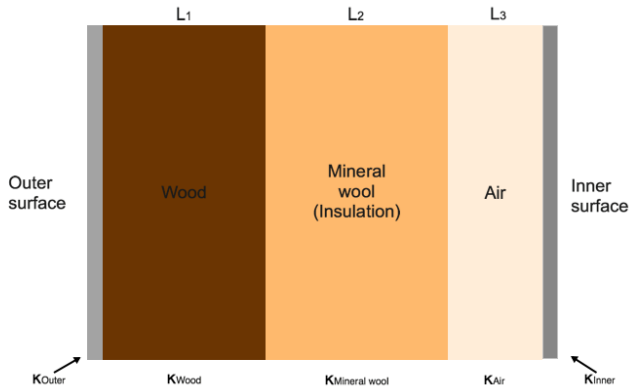

Figure 2.3: Schematics of a wall with different layers of materials. The outer surface, wood, mineral wool, air and the inner surface, each with an individual thickness (L_1, L_2, L_3) and thermal conductivity (κ_{OS}, κ_{Wood}, κ_{MW}, κ_{Air}, κ_{IS}). Notice that the outer and inner surfaces have thicknesses of one unit length making the thermal conductance equal to the thermal conductivity.

Super insulating materials (SIMs)

There is no exact definition concerning super insulating materials (SIMs) that is agreed upon. However, an often used definition for a SIM, is a material exhibiting a thermal conductivity below 0.025 $[Wm^{-1}K^{-1}]$ at ambient conditions. Table 2.2 lists three materials fulfilling the definition of SIMs along with air.

Table 2.2: Thermal conductivity's of selected super insulation materials (SIM)[11][12][13].

Material:	Thermal conductivity (κ) $[Wm^{-1}K^{-1}]$
Air	0.026
Vacuum insulation panels (VIP)	0.004-0.007
Silica aerogles	0.015-0.020
Hollow silica nano-spheres (HSNS)	0.015-0.020

Vacuum insulation panels (VIP)

Vacuum insulation panels (VIP) consist of membrane walls preventing air or other gases to penetrate the wall (Figure 2.4) [13]. The heat flow through vacuum is extremely low and the thermal conductivity (Table 2.2) of VIP shows how effective this structure resists the flow of heat.

VIP is costly to construct since it needs to perfectly fit the area it insulates and cannot be manually modified without disrupting the membrane. Thus they must be custom made for each project. Furthermore, mechanical stress may damage the membrane wall destroying the vacuum inside the panel. The diffusion of gases through the membrane causes the thermal conductivity (κ) to increase with time. Currently, VIPs are rarely used due to the high cost, need for customisation and the skills required for installation.

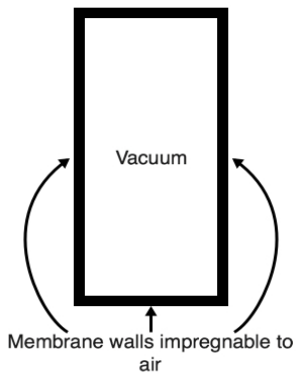

Figure 2.4: Structural illustration of vacuum insulating panels (VIP) [13].

Silica aerogels

Aerogels are porous materials generated from a gel, where the original liquid component has been replaced with a gas making them extremely light with a very low density. Silica aerogels (Table 2.2) consist of 90 $vol\%$ air and 10 $vol\%$ silica and the low thermal conductivity exhibited by the material is based on Knudsen diffusion as described later in section 2.4 [11].

2.3 Hollow silica nano spheres (HSNS)

Figure 2.5 illustrates the structure of the HSNS, where both the coating thickness and pore size varies greatly depending on synthesis method, concentration parameters and environmental conditions [14]. Similar to silica aerogels, HSNS exploit Knudsen diffusion as discussed later in section 2.4. In short, nano porosity combined with the low thermal conductivity of the silica network gives super insulating properties.

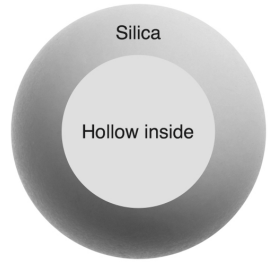

Figure 2.5: Cross - sectional illustration of a hollow silica nano-sphere

A disadvantage with HSNS is that the synthesised material are hydrophilic. Under wet conditions the HSNS would adsorb water, filling the hollow pores. Thus the low thermal conductivity with respect to diffusion of gases are replaced by water, considerably increasing the thermal conductivity. Originally, As - synthesised HSNS is a powder and would require a container or modifications to be integrated into a wall. Integrating a powder produces air holes and promotes a variation of density throughout the material. Modifications done on the HSNS to generate a more suitable insulation material would include integrating other components, altering the thermal conductivity. Ideally the spheres should be grafted together with flexible bonds without impairing the thermal properties.

2.4 Knudsen diffusion

Molecular diffusion

All particles above absolute zero (-273.15 $°C$) contain an internal energy resulting in thermal motion. This motion is the foundation of molecular diffusion which describes the net movement of particles from high to low concentrated areas [15]. Molecular diffusion is dependent on the density, temperature and the mass of the particles and are described using Fick's law of diffusion:

$$J_i = -D_i \nabla \varphi_i \tag{2.12}$$

Where J_i is the diffusion flux $[molm^{-2}s^{-1}]$, describing the amount of substance moving through a unit area over a unit time, D_i is the diffusion coefficient $[m^2s^{-1}]$ depending on the substance, $\nabla\varphi_i$ is the concentration gradient $[molm^{-3}]$ and i is the species of the substance.

Particles (molecules/atoms) will always strive to achieve the lowest possible energy state, prompting the flow of particles towards low concentration regions. Over time the concentration gradient goes towards zero as the particle flow generates a more uniform distribution.

Self - diffusion

Despite being in equilibrium the particles still contain thermal movement. This type of diffusion is described as self - diffusion and a substance in equilibrium has an altered molecular diffusion coefficient called the self - diffusion coefficient (D^*).

$$D_i^* = D_i \frac{\delta lnc_i}{\delta lna_i} \tag{2.13}$$

Where c_i is the concentration and a_i is the activity of the species i.

Molecular diffusion has a directional particle flow based on the concentration gradient . For self - diffusion the particle flow is described as random.

Kinetic theory of gases

The kinetic theory of gases describes gases as a large number of molecules with a constant motion. Each particle has a random movement direction occurring based on collisions with other particles along with the walls containing the gas. To describe this phenomenon the theory is based on the assumptions of ideal gases [16]:

1. The particles in the gas have identical mass and the total volume occupied by these particles is negligible. Stating that the distance between each particle is large compared to their size.
2. The particles are in constant, random movement and the particles are treated as perfectly elastic, indicating that structural changes based on collisions between them and the container walls are negligible.

3. Particle interactions are negligible except for collisions and the average kinetic energy depends only on the absolute temperature of the system.

Based on these assumptions a mathematical description of the self - diffusion coefficient for gases is given by.

$$D^*_{AA} = \frac{\lambda}{3}\sqrt{\frac{8RT}{\pi M_A}} \tag{2.14}$$

Where D^*_{AA} is the self - diffusion coefficient between the species A $[m^2 s^{-1}]$, λ is the mean free path between collisions $[m^{-1}]$, R is the gas constant $[Jmol^{-1}K^{-1}]$ and T is the temperature $[K]$.

Mean free path

The mean free path (λ)in gases is the average distance a particle moves before it collides with another particle. The distance is dependent on the species, the pressure and the temperature of the system. Table 2.3 shows the pressure dependency of the mean free path of air at room temperature.

Table 2.3: Mean free path of air (λ_{air}) for different pressure conditions at room temperature.

Conditions	Pressure ($mbar$)	Molecules per m^3	Mean free path (λ_{air})
Ambient Pressure	1013	2.7×10^{25}	68 nm [17]
Low vacuum	300-1	10^{25} - 10^{22}	0.1 - 100 μm
High vacuum	10^{-3} -10^{-7}	10^{19} - 10^{15}	10 cm - 1 km

Knudsen diffusion

Gases contained in large pores would have self-diffusion dominated by gas particle collisions. A pore size similar or smaller than the mean free path of the gas would result in a larger probability for a gas particle to collide with the pore wall rather than another gas particle. This phenomenon is called Knudsen diffusion and makes the diffusion dependent on the pore diameter rather than the mean free path.

$$D^*_{KA} = \frac{d}{3}\sqrt{\frac{8RT}{\pi M_A}} \tag{2.15}$$

Where D^*_{KA} is the Knudsen diffusion coefficient $[m^2 s^{-1}]$ and d is the pore diameter $[m]$.

The thermal conductivity drop achieved in Knudsen diffusion is related to the energy transfer between a gas molecule colliding with another gas molecules in contrast to a gas molecule colliding with a solid pore wall. The energy transferred in a gas/pore wall collision is considerably less efficient than a gas/gas collision, especially with a pore wall consisting of a nano-porous silica network. Scientific experiments done by Malek et al.[18], Johansson et al.[19] and Jelle et al.[20] have shown that achieving Knudsen diffusion drastically reduces the thermal conductivity of materials. Jelle et al.[20] demonstrated that the conductivity decreases for hollow silica nano-spheres with a pore diameter smaller than the mean free path of air λ_{air} [17].

2.5 Sample preparation

Polymerisation of templates

Nano-spherical polystyrene templates are the foundation for producing hollow silica nano spheres. These polystyrene templates are synthesised via emulsion polymerisation which branches from radical polymerisation [21]. Radical polymerisation is based on free radicals, acting as the initiators for the reaction. Styrene, the main reactant and monomer of the polymerisation of polystyrene, contains a vinyl group which can be broken by radicals. Potassium persulfate (KPS) is a common free radical generator and often used for radical polymerisations, including polymerisation of polystyrene. Dissolved KPS generates radicals with enough energy to break the π - bond in the vinyl group of styrene. Figure 2.6 illustrates the chemical dissolution of KPS. Notice that the reaction requires an aqueous solution and temperature above 50 $^\circ C$.

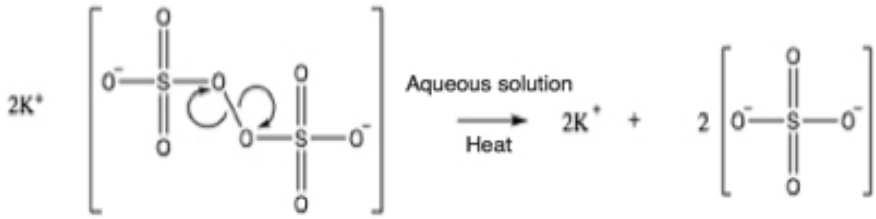

Figure 2.6: Reaction mechanism of the dissolution of potassium persulfate (KPS), in an aqueous solution at an elevated temperature [22].

Figure 2.7 illustrates the breaking of the π - bond in the vinyl group of styrene. R symbolises dissolved KPS acting as the free radical, initiating the process. Once the π - bond is broken the styrene molecule becomes unbalanced and the molecule immediately searches for possibilities to neutralise itself.

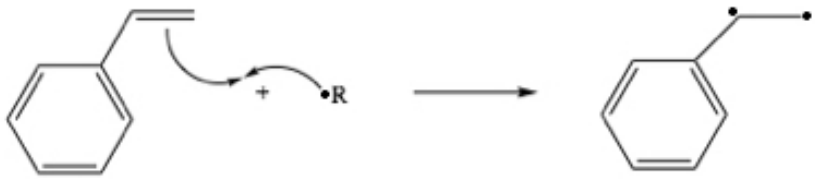

Figure 2.7: Illustration of free radicals breaking the π- bond in the vinyl-group of styrene. R symbolises dissolved KPS. [21]

When the propagation step of the polymerisation process is initiated, the unbalanced styrene molecule reacts with a styrene molecule attaching itself on the vinyl group by breaking it. The newly generated molecule would still be unbalanced and will continue reacting with styrene molecules in the same way.

Figure 2.8 illustrates the propagation processes occurring during the radical polymerisation of polystyrene.

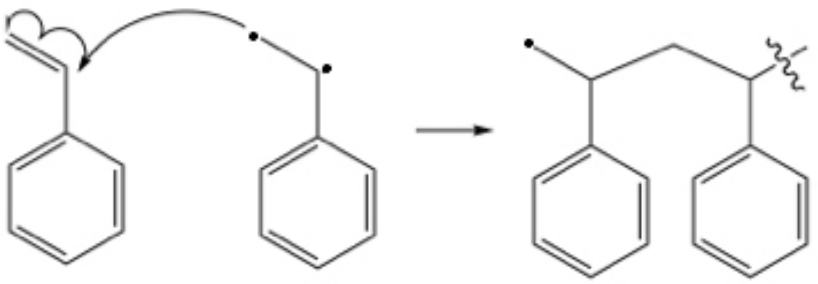

Figure 2.8: Illustration of the propagation process of radical polymerisation of polystyrene [21].

A radical polymerisation of polystyrene does not generate the necessary nano - spherical structure for further synthesis of hollow silica nano spheres. Emulsion polymerisation applies the same concept during polymerisation. The only key difference is the use of a surfactant [23]. During the polymerisation of polystyrene the surfactant functions as a dispersant, limiting the propagation of polystyrene.

A common surfactant for emulsion polymerisation of polystyrene is polyvinyl - pyrrolidone (PVP) illustrated in Figure 2.9. The surfactant generates nano-spherical polystyrene with a uniform distribution. Table 2.4 lists experimental results achieved by Sandberg et al.[24] relating the ratio between styrene, PVP and the diameter of the polystyrene particles synthesised.

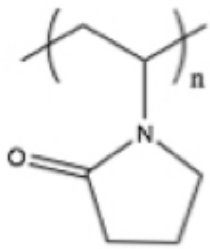

Figure 2.9: Chemical structure of polyvinylpyrrolidone (PVP) [25].

Table 2.4: Average diameter of the polystyrene spheres based on the ratio between PVP and styrene [24].

PVP-styrene ratio	Average diameter (nm)
0.0050	900 ± 30
0.0075	475 ± 4
0.010	355 ± 6
0.050	281 ± 1
0.10	228 ± 1
0.15	178 ± 1

Attaching silica nano particles on the template surface

An alkoxysilane, tetraethyl orthosilicate (TEOS) (Figure 2.10) is one possible precursor to produce silica nano particles suitable to attach themselves to the surface of the polystyrene templates. The compound undergoes a hydrolysis process, but generates a immiscible solution, which would produce a non- uniform coating profile.

Adding a homogenising agent such as 96 % ethanol would greatly enhance the miscibility of TEOS, providing a uniform coating profile [22].

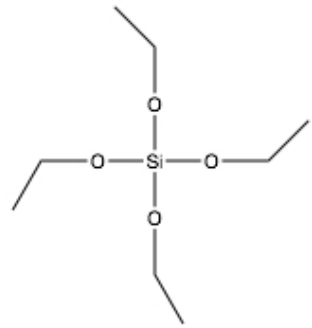

Figure 2.10: Chemical structure of tetraethyl orthosilicate (TEOS) [26].

Figure 2.11 is a miscibility diagram between TEOS, water and ethanol indicating that the solution during the coating process should consist of 80 % or more ethanol. Combined, TEOS and water should make up less than 20 % of the solution with a preferred ratio of 1:1.

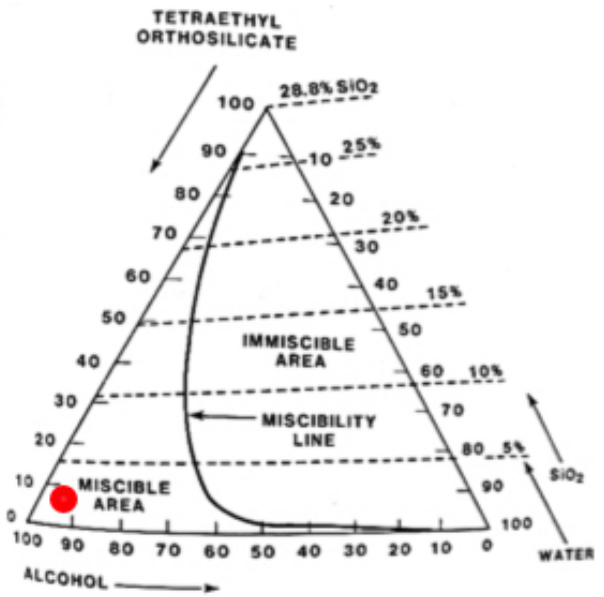

Figure 2.11: Diagram illustrating the miscibility between tetraethyl orthosilicate (TEOS), ethanol and water. The red area symbolises the concentration profile for an optimal synthesis of HSNS [22].

The coating process consists of two main reactions. A hydrolysis reaction and a condensation reaction.

Figure 2.12 is an illustration representing the hydrolysis of the TEOS molecules. One or more of the oxygen - silicon bonds in the TEOS molecule reacts with water producing a hydrolysed TEOS molecule and ethanol as a by - product. Once a hydrolysed TEOS molecule is produced, two different condensation reactions are possible. The two condensation reactions represented in Figure 2.13 and 2.14, attach two TEOS molecules, but produce two different by - products (ethanol and water, respectively).

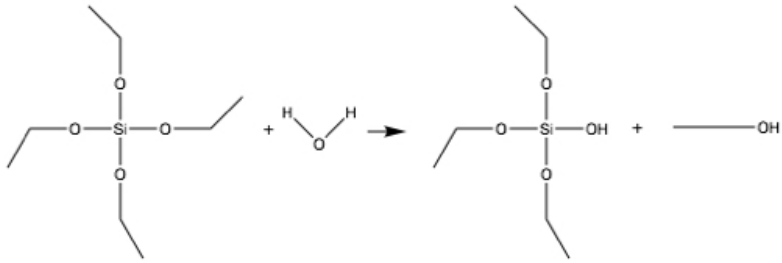

Figure 2.12: Hydrolysis reaction between TEOS and water [27].

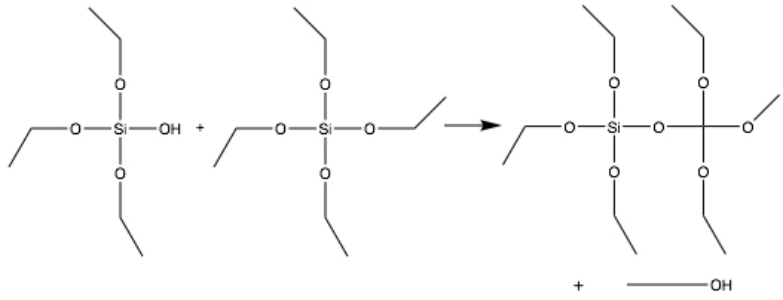

Figure 2.13: TEOS-condensation reaction binding two TEOS molecules together and forming ethanol as a by-product [27].

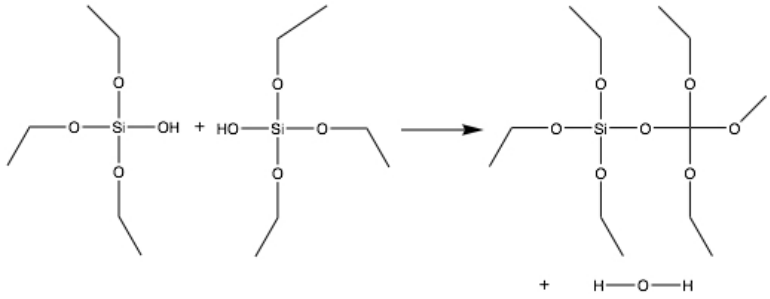

Figure 2.14: TEOS-condensation reaction between two hydrolysed TEOS molecules attaching them, forming water as a by-product [27].

The use of either acidic or basic catalysts would greatly enhance the reaction rate of the hydrolysis reaction. However, the use will affect the structural outcome of the silica particles. Table 2.5 lists the gelation time using either no, a basic or an acidic catalyst Table 2.6 shows the structural dependency based on the catalyst and concentration.

Table 2.5: Gelation time of silica with no catalyst, HCl and NH_4OH [22].

Catalyst	TEOS (mol/L)	pH	Time (h)
HCl	0.05	0.05	92
NH_4OH	0.05	9.95	107
No catalyst	0.05	5	1000

Table 2.6: Sol compositions for different silica - structures [22].

Silica - structures	TEOS ($mol\%$)	EtOH ($mol\%$)	H_2O ($mol\%$)	HCl ($mol\%$)	NH_3 ($mol\%$)
Fibers	11.4	77	11.4	0.2	-
Films	5.5	36	58	0.5	-
Mono dispersed spheres	4	86-87	4	-	5-6

After condensation the generated silica particles attach themselves on to the polystyrene surface, producing a coating thickness between 20 and 80 nm [14].

Heat treatment

A large difference in decomposition temperatures between silica and polystyrene, prompts the removal of polystyrene templates by heat treatment. Annealing at 500 $^\circ C$ for five hours decomposes and removes the polystyrene templates, producing the characteristic hollow structure. A side effect caused by the heat treatment is the removal of hydroxide groups from the surface of the silica particles. It has also been documented that heat treatment of silica above 400 $^\circ C$ modifies the surface reducing its abilities to rehydrate in water vapour [28].

2.6 Surface modification

The brittle and hydrophilic properties of as - synthesised HSNS are not practical for insulation materials. Modifying the silica surface to alter its properties is one solution to produce a material suitable for insulation. One of the surface modifications, hydrophobisation, focus on generating a hydrophobic material, while functionalisation, attaches functional groups that can be further used to connect the particles together into a monolith. Both processes produce a non - reversible surface alteration indicating that only one processes can be preformed.

Based on the removal of hydroxides and the reduced rehydration rate in water vapour after heat treatment. The silica surface needs to be hydroxylated before either functionalisation or hydrophobisation can occur.

Hydroxylation

By submerging the as - synthesised HSNS in an aqueous solution with a basic environment, the rate of hydroxylation would increase compared to hydroxylation of water vapour in air. A basic environment is preferred with respect to the increase of hydroxide formation on the surface. Figure 2.15 illustrates the hydroxylation processes on the heat treated silica surface, in an aqueous solution with a basic catalyst.

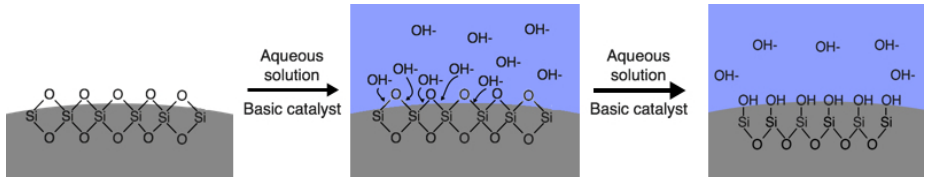

Figure 2.15: Hydroxylation of a silica surface, previously heat treated above 400 $^{\circ}C$.

Hydrophobisation

Silica's ability to adsorb water has a negative impact on the thermal resistance (R), under wet conditions [29]. A HSNS material exhibiting hydrophobic properties would remove the increase in thermal conductivity under wet conditions. A surface modification route developed by A. Hoseini et al. [30] has shown

that the use of 20 % - 30 % hexamethyldisiloxane (HMDS)(Figure 2.16) in n - heptane on silica aerogels, modifies the surface of the silica by increasing the hydrophobicity.

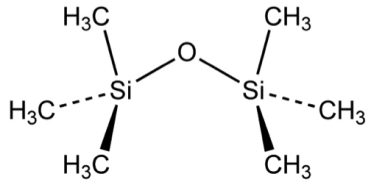

Figure 2.16: Chemical structure of hexamethyldisiloxane (HMDS) [31].

Figure 2.17 illustrates a unwanted reaction with HMDS, occurring with the presence of water. Air - dried hydroxylated HSNS consists of small amounts of water and these contaminants need to be removed. Washing the hydroxylated HSNS first in 100 % ethanol and then in n -heptane at an elevated temperature, the remaining water are completely removed [30]. Submerging the washed HSNS material in 20 % - 30 % HMDS at an elevated temperature the surface is modified.

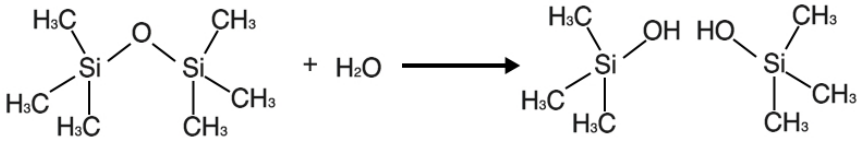

Figure 2.17: Unwanted chemical reaction between HMDS and water [30].

Illustrated in Figure 2.18 are the chemical reactions occurring during hydrophobisation. (a) represents the as - synthesised HSNS surface, (b) is an intermediate step and (c) represents the silica surface after hydrophobisation. The methyl groups from HMDS attaches itself to the silica surface, increasing the hydrophobicity.

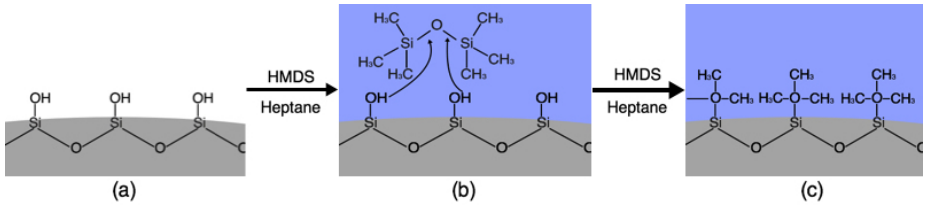

Figure 2.18: Illustration of the surface interaction occurring during hydrophobisation.

Functionalisation

The brittle structure of as - synthesised HSNS makes it less suitable for insulation purposes and combining the spheres through bridging organic groups will reduce the brittleness of the final insulation material. The use of vinyltrimethoxysilane (VMOS) (Figure 2.19) is one option in modifying the surface and connecting the separate spheres. The functionalisation process consists of two steps.

1. Grafting $C = C$ bonds to the surface of the silica.
2. Breaking the double bonds connecting the spheres.

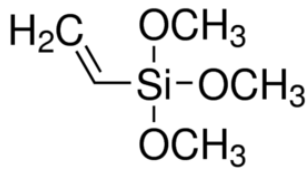

Figure 2.19: Chemical structure of vinyltrimethoxysilane (VMOS) [32].

Similar to the hydrophobisation process, the functionalisation process changes the hydrophobicity of the HSNS. VMOS consists of organic groups with a higher hydrophobicity than that of hydroxyl groups enhancing hydrophobic properties. Figure 2.20 illustrates the surface modification. VMOS reacts with the hydroxide - groups on the surface of the silica (b), attaching the VMOS molecule with a silica - oxygen bond. The surface modification generates two possible outcomes:

1. The remaining organic groups undergoes a reaction, bridging the VMOS molecules along with having $C = C$ bonds sticking out of the surface (c) .
2. The remaining organic groups undergoes no further reaction, producing a surface with $C = C$ bonds and large organic groups (d).

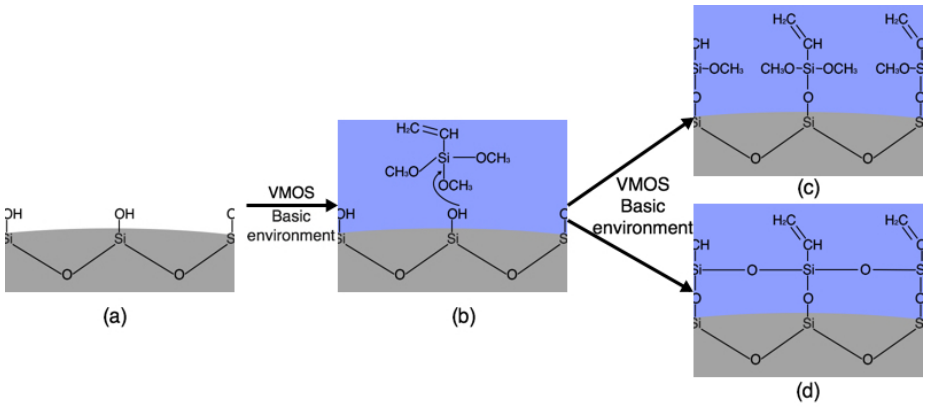

Figure 2.20: Illustration of the surface interactions occurring during functionalisation. Where (a) is the surface after hydroxylation, (b) is an intermediate step of the functionalisation and (c) and (d) are two possible outcomes of the functionalisation, where (d) produces a more hydrophobic surface.

2.7 Contact angle (θ)

The contact angle measured when a solid surface meets the liquid interface is called the contact angle (θ) . The θ quantifies the wettability of the solid material via the Young Equation 2.16 assuming an ideal surface [33]:

$$\gamma_{SG} = \gamma_{SL} + \gamma_{LG} cos(\theta) \tag{2.16}$$

Where γ_{SG}, γ_{SL} and γ_{LG} are the surface energies of the three phases, respectively, SL represents the surface in contact with the liquid and SG represents the surface in contact with gas, LG represents the line between the liquid and gas interface and θ represents the angle between LG and SL (contact angle). Based on the assumption of an ideal surface both the surfaces (SL and SG) are completely smooth. Listed in Table 2.7 is the wettability of a solid material

with respect to the contact angle (θ) and Figure 2.21 illustrates the apparatus for a contact angle measurement device.

Table 2.7: Wettability of a material with respect to the contact angle (θ) [33].

Contact angle (θ)	Wetabillity
$0°$	Complete wetting Super hydrophilic
$0° < \theta < 90°$	High wettability Hydrophilic
$90° < \theta < 150°$	Low wettability Hydrophobic
$150° < \theta < 180°$	Extremely low wettability Super hydrophobic
$180°$	Non-wetting

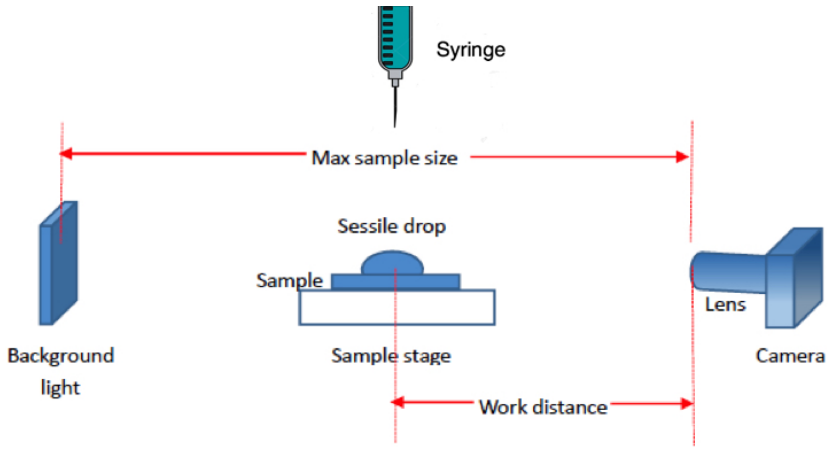

Figure 2.21: Illustration of a contact angle measurement apparatus: It consists of a high powered camera, a sample carrier, a syringe for deposition of liquids and a background [33].

An ideal surface is hard to achieve and deviations would generate an error on the contact angle. The error occurring can be measured by comparing both

connection points. Figure 2.22 illustrates a case where the surface of the solid material has been tilted, producing a non - ideal surface. This generates two different contact angles θ_{max} and θ_{min}, where $\theta_{max} > \theta_{min}$ since gravity drags the droplet in one direction. When measuring non-wetting (super hydrophobic) materials (Table 2.7) an ideal surface is essential to avoid the droplet to roll of the solid surface [34].

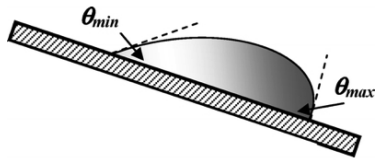

Figure 2.22: Illustration of a contact angle measurement done on a tilted surface, generating a un - symmetrical droplet of the liquid [34].

2.8 Thermal conductivity (Hot disk)

Thermal conductivity measurements done with a Hot disk transient plane source (TPS) are able to determine conductivities of insulation materials with a acceptable uncertainty. Figure 2.23 illustrates the apparatus of a TPS, consisting of a Hot disk sensor (a), a top and bottom sample holder with a specific cross - sectional area (b), a top and bottom stainless steel plate (c), a compressive load holding the cell together (d) and a cover (e). Figure 2.24 illustrates the heat flow occurring during the measurement, where the material measured experiences energy from an applied heat source. Dependent on the measurement parameters the amount of energy applied during a unit time ($\frac{Q}{\Delta t}$) and the cross - sectional area (A) of the material is specified [35].The analysing program of the hot disk apparatus determines the temperature difference (ΔT) between x_{start} (a point on the top sample compartment) and x_{end} (a point on the bottom sample compartment) by using the hot disk sensor positioned between the two points. Rearranging the Equation 2.4 with respect to the thermal conductivity (κ), provides the following expression.

$$\kappa = \frac{Q\Delta x}{A\Delta t\Delta T} \tag{2.17}$$

All variables are either defined or determined by the Hot disk transient plane source (TPS) analysing program except for the thermal conductivity (κ). Hence the thermal conductivity of the material measured can be calculated.

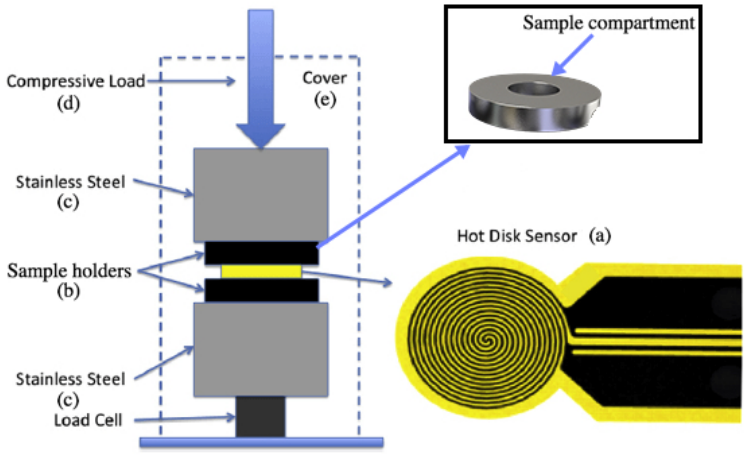

Figure 2.23: Illustration of a Hot disk transient plane source (TPS) apparatus [36].

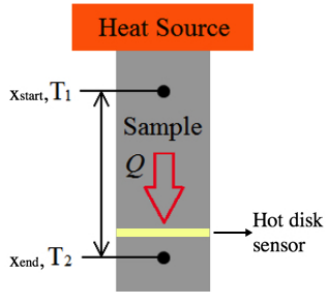

Figure 2.24: Illustration of the heat flow during a Hot disk TPS measurement. The energy applied increases the internal energy of the sample, dependent on its thermal conductivity [35].

Chapter 3

Experimental work

3.1 Sample nomenclature

Figure 3.1 illustrates the nomenclature of the hollow silica nano sphere samples after synthesis and surface modifications. This nomenclature is used throughout the text.

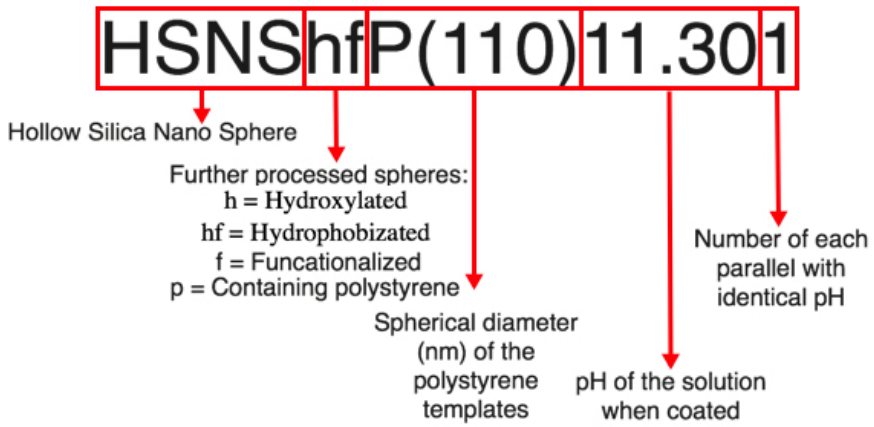

Figure 3.1: Nomenclature of the hollow silica nano spheres samples.

3.2 Chemicals

Listed in Table 3.1 are all chemicals used during preparation and surface modifications of HSNS.

Table 3.1: Chemicals used during preparation and surface modification of HSNS.

Chemical:	Abbreviation:	State:	Cons: (%)	Producer:
Styrene	-	(l)	99	Sigma Aldrich
Polyvinylpyrrolidone	PVP	(s)	-	Sigma Aldrich
Potassium persulfate	KPS	(s)	-	Sigma Aldrich
Ethanol	EtOH	(l)	96	Sigma Aldrich
Ethanol	EtOH	(l)	99.8	Sigma Aldrich
Tetraethyl orthosilicate	TEOS	(l)	99	Sigma Aldrich
Ammonium hydroxide	NH_4OH	(l)	25-30	Sigma Aldrich
n -heptane	-	(l)	99	Sigma Aldrich
Hexamethyldisiloxane	HDMS	(l)	99	Sigma Aldrich
Vinyltrimethoxysilane	VMOS	(l)	99	Sigma Aldrich
Distilled water	-	(l)	100	NTNU
Hydrochloric acid	HCl	(l)	25	Sigma Aldrich

3.3 Preparation of hollow silica nano-spheres

Emulsion polymerisation of polystyrene nano particles and coating of silica nano particles were conducted based on the experimental procedure developed by Sandberg et al. [24].

Nano - spherical polystyrene templates

PVP (1.5 g) was dissolved in distilled water (100 g) in a 250 mL beaker using magnetic stirring. Styrene (10 g) was added and stirred at 500 rpm for 15 min. Thereafter potassium persulfate (KPS) (0.16 g) was dissolved in distilled water (10 g) and added drop wise to the main solution. The solution was submerged into a oil bath at 70 $^{\circ}C$ for 24 hours under constant stirring. Provided in Appendix B is a detailed experimental overview over each polymerisation, listed in Table B.2.

Coating of silica nano particles

Polystyrene templates were uniformly distributed by magnetic stirring for 15 min at 500 rpm in 96 % EtOH. Thereafter the basic catalyst, concentrated ammonia solution (NH_4OH) or acidic catalyst (HCl), was added via titration, where the amounts (1-10 mL) depended on the desired pH in each synthesis. Tetraethyl ortosilicate (TEOS) was then physically mixed with distilled water at a 1:1 ratio and drop wise deposited to the main solution. Afterwards the solution was magnetically stirred at 500 rpm in ambient temperature for 24 h, before the sample was centrifuged (8000 rpm, 10 min) and the decanted. The solid material was dried in room temperature for 24 h before further processing. Table 3.2 lists an experimental overview of all synthesised HSNS, catalysed with a basic catalyst. All synthesised HSNS catalysed with an acidic catalyst is given by Table B.3 in Appendix B.

Heat treatment

The polystyrene was removed from the as - synthesised HSNS by heating the material to 500 $^{\circ}C$ and keeping the temperature constant for 5 h.

3.4 Surface modification

Hydroxylation

Heat treated HSNS was submerged in distilled water (20 mL) and concentrated ammonia solution (NH_4OH) (15 drops). To avoid evaporation the beaker was covered with a lid to generate a semi-closed container and the material was left to hydroxylate for three days.

Hydrophobisation

The hydrophobisation process was conducted based on the experimental procedure developed by Einarsrud et al.[30]. Hydroxylated HSNS were washed with 100 % EtOH four times over 24 h at 60 $^{\circ}C$ and then n - heptane four times over 24 h at 60 $^{\circ}C$. After each washing process the remaining n -heptane/EtOH was extracted by a pipette. Thereafter the HSNS were dispersed in 30 % HMDS in n -heptane (10 mL) at 60 $^{\circ}C$. To avoid evaporation the suspension was covered with a plastic lid and left to react for 24 h. The liquid was extracted by a pipette and the material was washed four times over 24 h with n - heptane at 60 $^{\circ}C$.

Table 3.2: Experimental overview for all synthesised HSNS catalysed with a basic catalyst.

Nr:	Sample:	Polystyrene (g)	EtOH (mL)	NH_4OH (mL)	pH	TEOS -sol (mL)	Yield (g)
1	HSNSpP(160)11.191	12.02	200	3.4	11.19	16	0.974
2	HSNSpP(160)11.261	12.00	200	4.0	11.26	16	0.890
3	HSNSpP(140)11.301	6.01	120	1.45	11.30	10	Not tested
4	HSNSpP(140)11.302	6.00	120	1.50	11.30	10	Not tested
5	HSNSpP(160)11.303	6.01	120	2.6	11.30	10	Not tested
6	HSNSpP(160)11.304	6.03	120	2.6	11.30	10	Not tested
7	HSNSpP(160)11.401	6.02	120	2.5	11.40	10	0.494
8	HSNSpP(160)11.461	9.95	200	7.0	11.46	16	1.879
9	HSNSpP(160)11.491	6.94	150	6.0	11.49	14	1.125
10	HSNSpP(160)11.501	6.01	120	3.1	11.50	10	1.470
11	HSNSpP(160)11.502	6.02	120	3.5	11.50	10	1.816
12	HSNSpP(160)11.551	6.00	120	4.0	11.55	10	1.442
13	HSNSpP(160)11.601	6.01	120	9.8	11.60	10	Not tested
14	HSNSpP(160)11.651	6.06	120	6.0	11.65	10	1.394
15	HSNSpP(160)11.701	6.01	120	4.7	11.70	10	1.482
16	HSNSpP(160)11.702	6.02	120	5.8	11.70	10	1.698
17	HSNSpP(160)11.761	6.04	120	8.0	11.76	10	1.090
18	HSNSpP(160)11.901	6.02	120	7.2	11.90	10	1.574
19	HSNSpP(160)11.902	6.01	120	7.5	11.90	10	1.448
20	HSNSpP(140)12.001	6.02	120	3.4	12.00	10	Not tested
21	HSNSpP(140)12.002	6.01	120	3.4	12.00	10	Not tested

Functionalisation

Hydroxylated HSNS were dispersed by magnetic stirring in 96 % EtOH (50 - 100 mL). A basic environment similar to the coating process was generated by addition of concentrated ammonia solution (NH_4OH) (1 - 4 mL). Thereafter VMOS (1 - 3 mL) was deposited drop wise to the mixture and left to react for 24 h with constant magnetic stirring at 500 rpm. The solution was then centrifuged (8000 rpm, 20 min) and the solid material was left to dry in air for 24 h. The amounts of chemicals necessary in the functionalisation process is dependent on the yield and the pH of the coating process. Table 3.3 lists the experimental overview of all functionalised HSNS samples. The volumetric parameters vary greatly between the functionalised HSNS samples. E.g HSNSf(140)11.462 vs HSNSfpP(140)11.501.

3.5 Sample characterisation

After each processing step, an small amount of the HSNS materials was put aside to characterise the samples.

Structural characterisation

Sample morphology was analysed using a Hitachi FlexSEM 1000 scanning electron microscope (SEM) at an electron voltage of keV[37]. The microscope produced topographical micrographs with an acceptable resolution at a magnification of $\times 50$. Before each scan the samples were dispersed in 96 % EtOH and dropped on to an aluminium sample carrier. The material was coated with gold (Au) using a Cressington sputter coater 108auto.

Component characterisation

To analyse the presence of chemical components Fourier - transform infrared spectroscopy (FTIR) was used (Nicolet 8700 with an ATR measuring diamond). For each measurement the sample powder was added on the diamond surface, completely covering it. The material was then pressed on to the ATR diamond by using the blunt arrowhead attached to the device.

Table 3.3: Experimental overview of all functionalised HSNS samples. Notice the large variations in concentration parameters.

Sample name:	Sample used:	(g)	EtOH (mL)	NH_4OH (mL)	pH	VMOS (mL)
HSNSfP(160)11.401	HSNSP(160)11.401	0.231	50	2.0	Not tested	2.0
HSNSfP(160)11.461	HSNSP(160)11.462	1.865	250	8.0	11.45	12.0
HSNSfpP(160)11.501	HSNSpP(140)11.501	0.034	40	1.0	11.40	1.0
HSNSfP(160)11.501	HSNSP(160)11.501	0.135	40	2.0	11.00	1.2
HSNSfpP(160)11.502	HSNSpP(160)11.502	0.026	40	1.5	11.10	1.0
HSNSfP(160)11.502	HSNSP(160)11.502	0.179	50	2.0	11.24	1.2
HSNSfP(160)11.551	HSNSP(160)11.551	0.549	75	3.5	Not tested	3.0
HSNSfP(160)11.651	HSNSP(160)11.652	0.499	75	3.9	Not tested	3.0
HSNSfP(160)11.761	HSNSP(160)11.762	0.403	75	5.6	Not tested	3.0

Hydrophobicity analysis

The hydrophobicity of hydroxylated and functionalised HSNS samples were analysed using the drop shape analyser DSA 1000. Each sample was placed in a sample holder with a diameter of 2 *cm* and a hight of 2 *mm*. Furthermore the material was pressed together to generate an ideal surface using an aluminium plate.

Thermal conductivity analysis

The Hot disk transient plane source TPS 2500 instrument was used to measure and compare the thermal conductivity of the heat treated and functionalised HSNS samples. The sample was deposited into two sample holders with a diameter of 1 *cm* and a height of 1 *cm*. Furthermore the material was pressed with an equal amount of pressure on both sample holders to generate equal surfaces and densities.

Chapter 4

Results

4.1 Polystyrene

Morphology

The SEM micrographs in Figure 4.1 display two polystyrene batches used for further preparation of hollow silica nano-spheres. Both batches exhibit the wanted nano-spherical structure with a uniform size distribution throughout the material. Sphere size measurements done on the SEM micrographs in Figure 4.1 and Figure C.1 in Appendix C, provided an average diameter of the polystyrene batches. The average diameter of P(140) was measured to 140 $\pm$ 12.5 nm and P(160), 160 $\pm$ 15 nm. Table 4.1 lists size measurements done on different spheres throughout all four SEM micrographs.

Composition

The FTIR spectra of the polystyrene batches P(140) and P(160) are illustrated in Figure 4.2 a and b respectively. Both FTIR spectra exhibit a strong band at 700 cm^{-1} representing mono-substituted benzene. The three smaller bands between 1400 - 1750 cm^{-1} are attributed to aromatic $C = C$ bonds while the two bands between 2900-3100 cm^{-1} represents $C - H$ stretching vibrations. Comparing the two FTIR spectra with a reference spectrum of polystyrene (Figure A.1, Appendix [38]), the spectra resemble the reference spectrum.

Table 4.1: Sphere size measurements of the polystyrene batches P(140) and P(160), based on the SEM micrographs in Figure 4.1 and C.1. The variation in uncertainty is based on the magnification difference in the SEM micrographs.

Diameter: (Figure 4.1, (a)) (nm)	Diameter: (Figure C.1, (a)) (nm)	Diameter: (Figure 4.1,(b)) (nm)	Diameter: (Figure C.1, (b)) (nm)
140 ± 10	140 ± 15	170 ± 10	160 ± 20
130 ± 10	140 ± 15	160 ± 10	150 ± 20
150 ± 10	150 ± 15	150 ± 10	160 ± 20
140 ± 10	150 ± 15	170 ± 10	170 ± 20
140 ± 10	160 ± 15	150 ± 10	160 ± 20
150 ± 10	130 ± 15	140 ± 10	160 ± 20
130 ± 10	150 ± 15	150 ± 10	150 ± 20
130 ± 10	130 ± 15	160 ± 10	170 ± 20
140 ± 10	150 ± 15	170 ± 10	170 ± 20
Average:	Average:	Average:	Average:
138.8 ± 10	144.4 ± 15	157.7 ± 10	161.1 ± 20
Combined average:		Combined average	
141.6 ≈ 140 ± 12.5		159.4 ≈ 160 ± 15	

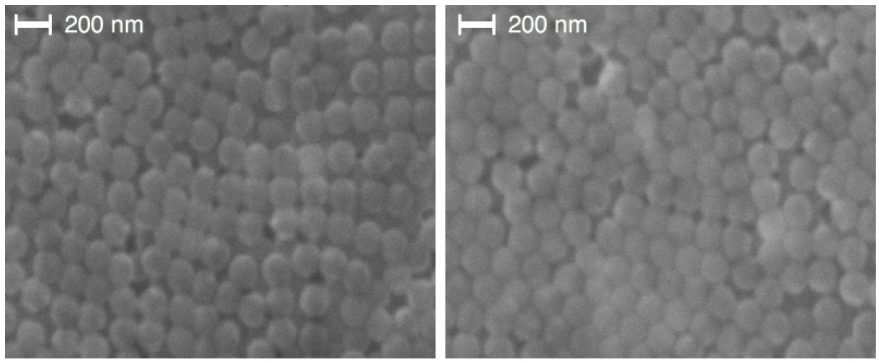

Figure 4.1: SEM micrographs of the polystyrene batches P(140) (a) and P(160) (b). Exhibiting a uniform distribution, a nano - spherical structure and an average diameter of 140 ± 12.5 nm and 160 ± 15 nm, respectively.

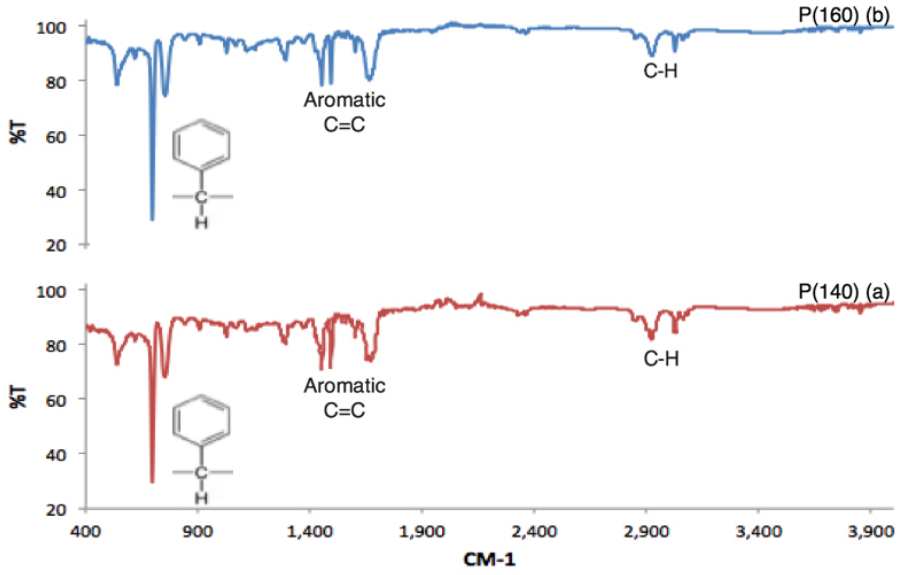

Figure 4.2: FTIR spectra of the two polystyrene batches P(140) (a) and P(160) (b).

4.2 Hollow silica nano- pheres

Overview

Silica coated polystyrene, as - synthesised and surface modified HSNS were characterised with respect to morphology, composition and hydrophobicity. The results are presented and compared in this chapter. Furthermore the thermal conductivity of HSNS before and after functionalisation is presented at the end of this chapter. Table 4.2 gives an overview of the layout of the results in regards to HSNS.

Table 4.2: Layout of the results describing HSNS.

Section:	Property described:	Preparation step:
4.2.1	Morphology	Silica coated polystyrene As - synthesised HSNS Hydroxylated, hydrophobisated and functionalised HSNS
4.2.2	Composition	Silica coated polystyrene As - synthesised HSNS Hydroxylated HSNS Functionalised HSNS
4.2.3	Hydrophobicity	Silica coated polystyrene, as - synthesised and hydroxylated HSNS Hydrophobisated HSNS
		Functionalised HSNS
4.4.4	Thermal conductivity	Functionalised and as - synthesised HSNS

4.2.1 Morphology

Silica coated polystyrene

Figure 4.3 represents SEM micrographs of the two silica coated polystyrene samples, HSNSpP(160)11.301 (Figure 4.3 (a)) and HSNSpP(160)11.302 (Figure 4.3 (b)). These two samples generated an unwanted morphology where the material produced large blocks rather than separate spheres. Figure 4.5 represents SEM micrographs of four silica coated polystyrene samples. HSNSpP(160)11.303 (Figure 4.5 (a)) has an average diameter of 220 nm with a silica coating of 40 nm around the 160 nm polystyrene templates. The coating consists of nano - particles of silica resulting in a porous surface layer. HSNSpP(160)11.501 (Figure 4.5 (b)) has an average diameter of 200 nm with a silica coating of 30 nm. HSNSpP(160)11.501 has a similar structure to that of HSNSP(160)11.303 consisting of nano - particles of silica covering the surface of the polystyrene. But comparing the agglomeration, these silica nano - particles are larger, resulting in a less porous surface of HSNSpP(160)11.501. HSNSpP(140)12.001 (Figure 4.5 (c)) has an average diameter of 180 nm with a silica coating of 35 nm. The coating consists of film of silica on the surface and the spheres are slightly agglomerated. Compared to HSNSpP(160)11.303 and HSNSpP(160)11.501, HSNSpP - (160)12.001 exhibits a less porous surface coverage. HSNSP(160)11.901 (Figure 4.5 (d)) shows a highly agglomerated HSNS sample with a particle size of around 600 nm and a film of silica covering the surface.

In regards to Knudsen diffusion, the morphology of HSNSpP(160)11.303 and HSNSpP(160)11.501 (a porous silica surface coverage), is the most suitable morphology to achieve the lowest thermal conductivity.

These samples have identical synthesis parameters except for the amount of ammonia solution added during the coating process (Table 3.2). Dependent on the amount of ammonia solution, the morphology of the HSNS materials changes drastically. Table 4.3 lists the morphology of the six silica coated polystyrene samples in terms of sphere diameter, silica coating thickness, porosity and agglomeration. Both HSNSpP(160)11.301 and HSNSpP(160)11.302 have an very small amount of ammonia solution added during the coating process (1.45 mL and 1.50 mL, respectively), while HSNSpP(160)11.303 and HSNSpP(160)11.501 have a moderate amount of ammonia solution (2.6 mL and 3.1 mL, respectively) added. HSNSpP(140)12.001 on the other hand, has a higher pH than all other five HSNS samples. However, only an amount of 3.4 mL of ammonia solution is

added. Lastly HSNSP(160)11.901 has the largest amount of ammonia solution (7.2 mL), but a lower coating pH than HSNSpP(140)12.001. Hence the microstructures of the silica coated polystyrene are not directly related to the pH of the coating solution, but rather to the amount of ammonia solution added. NH_3 evaporates in contact with air and repetitive use of the same bottle during each synthesis would result in the reduction of the NH_3 concentration and a relative increase of water. Based on a hypothesis developed, the same amount of a less concentrated solution of ammonia would still have the same reaction effect. However, the pH of the coating - solution would be lower.

Repetitive preparations in a pH range of 11 - 12, resulted in a structural outcome overview. Below 1.5 mL of NH_4OH - solution the coating synthesis generates large blocks rather than nano - particles. The most suitable morphology generation in regards to insulation was achieved by an addition of 1.5 - 3.0 $\pm$ 0.5 mL of NH_4OH - solution, producing silica nano - particles covering the surface of polystyrene templates. An addition of 3.5 - 5.0 $\pm$ 0.5 mL of NH_4OH - solution generates a film of silica on the surface. The spheres also have small tendency of agglomeration. An addition of $\geq$ 5.5 $\pm$ 0.5 mL of ammonia - solution produces agglomerated spheres with multiple polystyrene templates and a film of silica on the surface. Figure 4.4 illustrates the yield for as - synthesised HSNS with respect to the amount of ammonia - solution. The colour codes represented on each data point symbolise the pH of the coating process, explained in the top right corner of the figure. The plot is divided into three separate areas (a, b and c) representing the morphology change based on the amount of ammonia - solution added.

Table 4.3: Structural overview of the silica coated polystyrene samples: HSNSpP(140)11.301, HSNSpP(140)11.302, HSNSpP(160)11.303, HSNSpP(160)11.501, HSNSpP(140)12.001 and HSNSpP(160)11.901.

Sample:	Diameter (nm)	Silica (nm)	Porosity	Agglomeration
HSNSpP(140)11.301	Blocks	-	-	Extreme
HSNSpP(140)11.302	Blocks	-	-	Extreme
HSNSpP(160)11.303	220	40	High	None
HSNSpP(160)11.501	200	30	Moderate	None
HSNSpP(140)12.001	180	35	Low	Slight
HSNSpP(160)11.901	600	Variable	Low	High

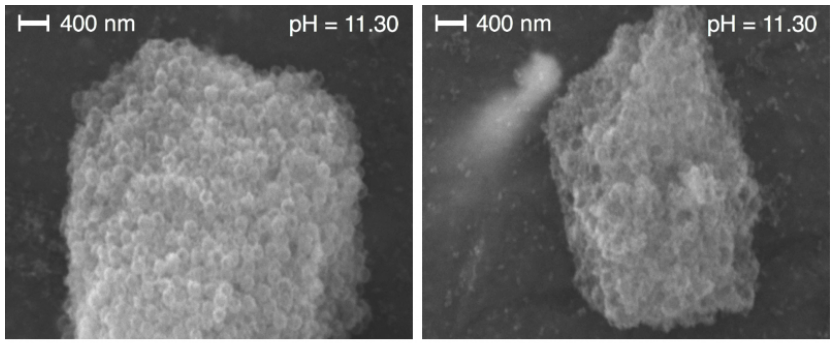

Figure 4.3: SEM micrographs of the silica coated polystyrene samples: HSNSP(140)11.301 (a) and HSNSP(140)11.302 (b). Notice the change in magnification.

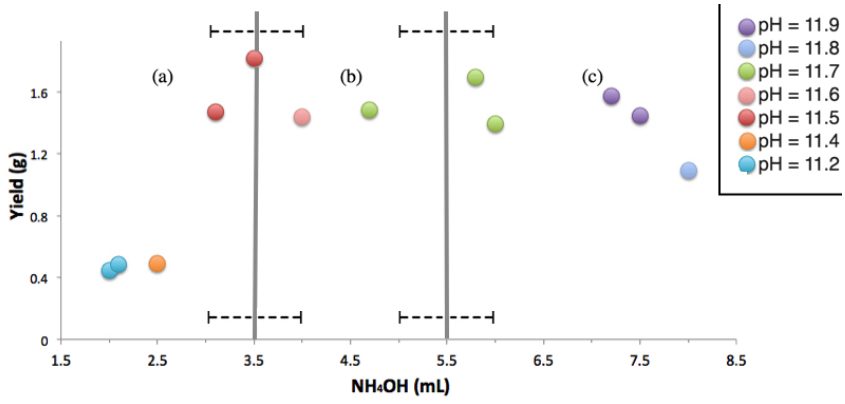

Figure 4.4: Yield and structural overview of HSNS materials prepared during this work. Area (a) represents the formation of a porous silica surface coverage with no agglomeration, (b) represents formation of a film of silica on the surface, along with a small tendency of agglomeration and (c) represents formation of highly agglomerated spheres, along with a film of silica covering the surface. The data points are sorted in different colours, where each colour represents a coating pH showed in the top right corner.

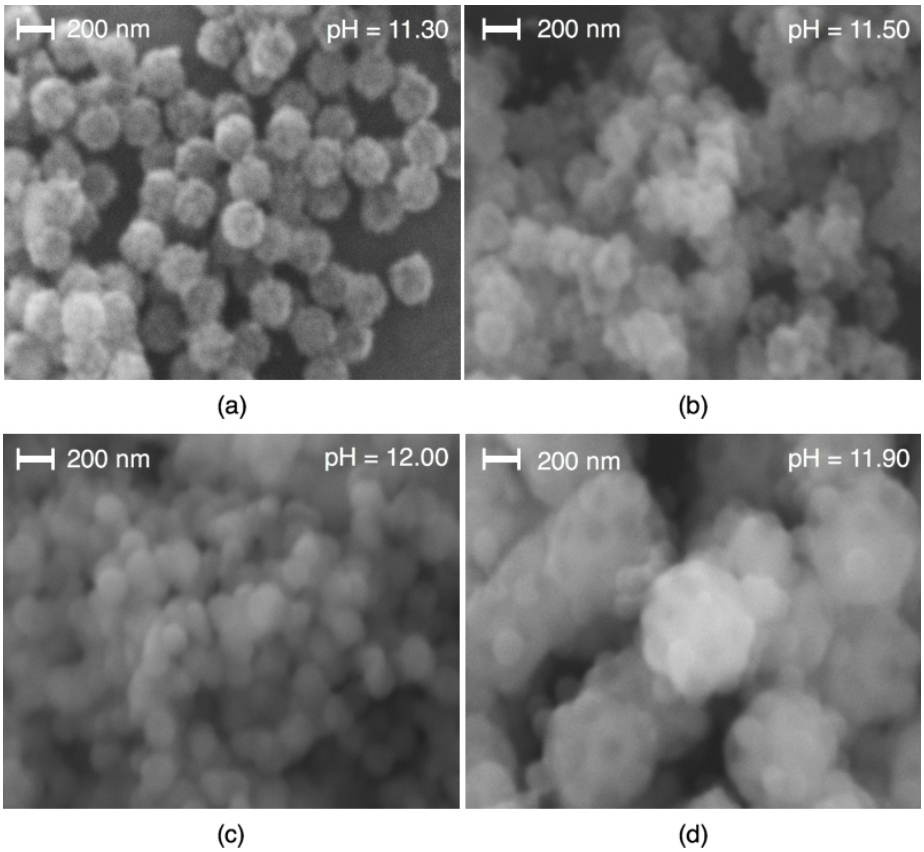

Figure 4.5: SEM micrographs of the silica coated polystyrene samples: HSNSpP(160)11.303 (a), HSNSpP(160)11.501 (b),HSNSpP(140)12.001 (c) and HSNSpP(160)11.901 (d)

Provided in Appendix C.1 are additional SEM micrographs in Figure C.2 and C.3 for silica coated polystyrene samples.

As - synthesised hollow silica nano spheres

The SEM micrographs in Figure 4.6 represent the same samples shown in Figure 4.5 after heat treatment. The morphology of the samples remains the same after heat treatment in terms of average diameter and silica coating thickness. The structural changes occurring are the silica surface coverage and the inner structure of the sphere. Table 4.4 lists the structural changes occurring during heat treatment. The two SEM micrographs of the HSNS samples: HSNSaP(140)12.001 (Figure 4.6 (c)) and HSNSP(160)11.901 (Figure 4.6 (d)) produced holes in the surface of the spheres during heat treatment. HSNSP(140)12.001 has one hole in each sphere, while HSNSP(160)11.901 has multiple holes in each agglomerated sphere. The porous HSNS samples: HSNS - P(160)11.303 (Figure 4.6 (a)) and HSNSP(160)11.501, (Figure 4.6 (b)) were not affected by heat treatment in regards to the silica surface coverage.

During heat treatment all HSNS samples prepared, generated the characteristic hollow structure. With respect to the SEM micrographs, confirmation of the hollow structure was only possible with HSNS samples with a film of silica covering the surface, e.g HSNSP(140)12.001 (c) and HSNSP(160)11.901 (d).

Hydroxylated, hydrophobisated and functionalised HSNS

The SEM micrographs in Figure 4.7 represent the hydroxylated HSNS sample, HSNShP(160)11.501 (Figure 4.7 (a)), the hydrophobisated HSNS sample, HSNShfP(140)12.001 (Figure 4.7 (b)) and the functionalised HSNS sample HSNSf - P(140)11.501 (Figure 4.7 (c)). The microstructure of all HSNS samples after hydroxylation, hydrophobisation and functionalisation remains unchanged compared to as -synthesised HSNS.

Table 4.4: Structural overview of the as - synthesised HSNS samples, HSNSP(160)11.303, HSNSP(160)11.501, HSNSP(140)12.001 and HSNSP(160)11.901.

Sample:	Generation of holes:
HSNSP(160)11.303	None
HSNSP(160)11.501	None
HSNSP(140)12.001	One hole in each sphere
HSNSP(160)11.901	Multiple holes in each agglomerated sphere

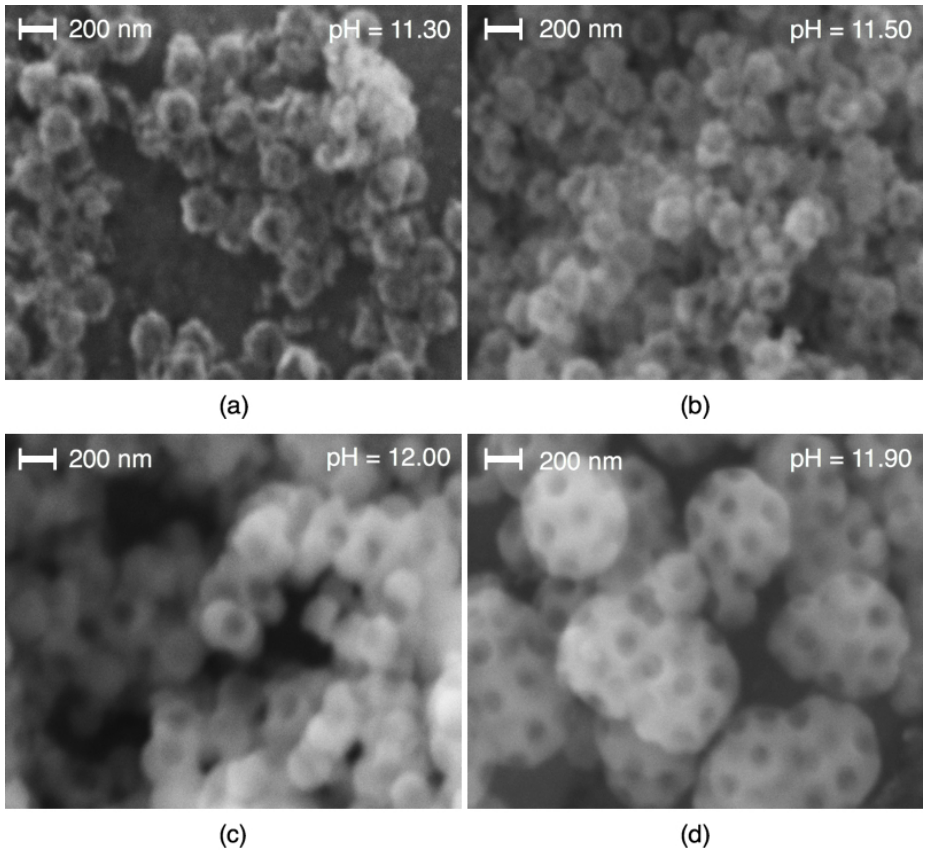

Figure 4.6: SEM micrographs of as - synthesised HSNS samples, HSNSP(160)11.303 (a), HSNSP(160)11.501 (b) ,HSNSP(140)12.001 (c) and HSNSP(160)11.901 (d)

Provided in Appendix C.1 are additional SEM micrographs in Figure C.4 and C.5 for as - synthesised HSNS samples.

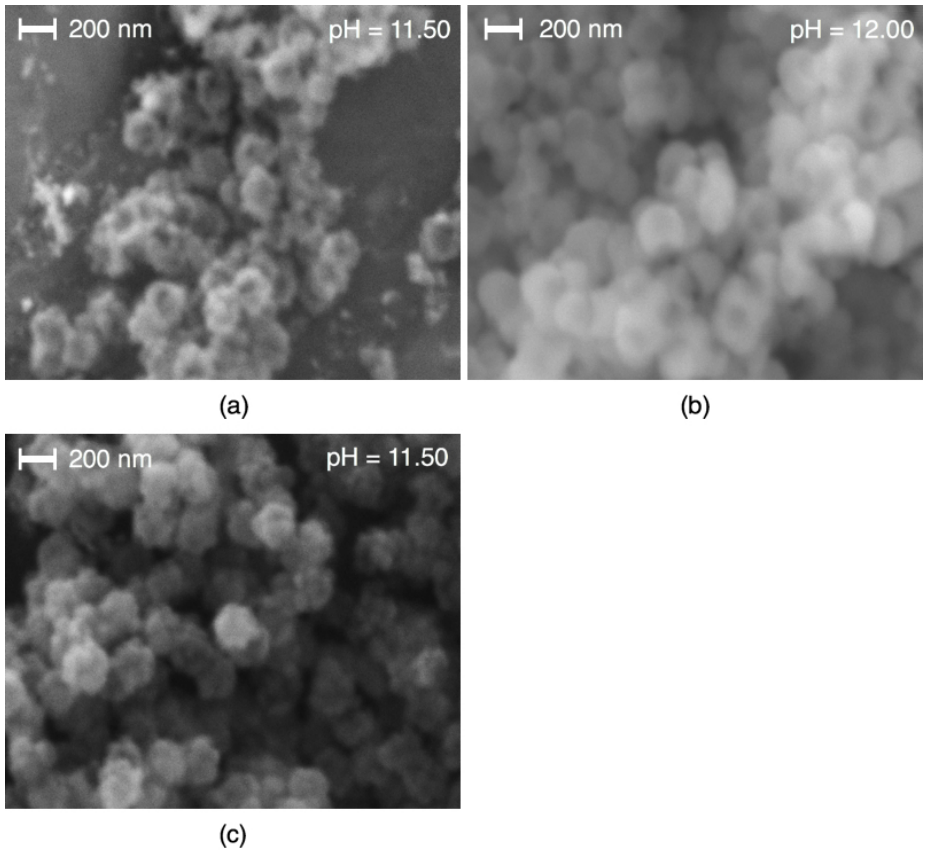

Figure 4.7: SEM micrographs of the hydroxylated HSNS sample, HSNShP(160)11.501(a), the hydrophobisated HSNS sample, HSNShfP(140)12.001 (b) and the functionalised HSNS sample, HSNSfP(160)11.501 (c).

Provided in Appendix C.1 are additional SEM micrographs for hydroxylated (Figure C.6 and C.7) and functionalised (Figure C.8) HSNS samples.

4.2.2 Composition

Silica coated polystyrene

FTIR spectra of the polystyrene spheres P(160) and the silica coated polystyrene sample HSNSpP(160)11.501 are displayed in Figure 4.8. During the coating process of HSNSpP(160)11.501, polystyrene templates of the batch P(160) were used, making it suitable to compare these two FTIR spectra. As previously mentioned in section 4.1 the polystyrene batch P(160) contains all three characteristics polystyrene IR - bands. By comparing the FTIR spectrum of HSNSpP(160)11.501 the characteristic polystyrene bands are also present, but with a lower intensity. The mono - distributed benzene band (700 cm^{-1}) and the aromatic $C = C$ bonds bands (1400-1750 cm^{-1}) are both highly noticeable, while the $C - H$ stretching vibration bands (2900-3100 cm^{-1}) are almost unidentifiable based on the presence of $H - O$ bonds dominating this part of the FTIR spectrum.

The attachment of silica nano - particles on to the polystyrene templates have been successful with respect to the characteristic silica bands in the FTIR spectrum of HSNSpP(160)11.501 (Figure 4.8, b). The three bands at 450, 800 and 1100 cm^{-1} represents $Si-O-Si$ bonds and the band at 900 cm^{-1} is attributed to $Si - OH$ bonds. Table 4.5 lists functional groups identified by comparing the two FTIR spectra with the polystyrene reference spectrum (Figure A.1, Appendix A) and the silica reference spectrum (Figure A.2, Appendix).

Table 4.5: Functional groups identified by a FTIR measurement of the two samples P(160) and HSNSpP(160)11.501.

Sample:	Functional groups identified (FTIR):
P(160)	Mono-substituted benzene (700 cm^{-1}) Aromatic C=C (1400-1750 cm^{-1}) C-H (2900-3100 cm^{-1})
HSNSpP(160)11.501	Si-O-Si (450, 800, 1100 cm^{-1}) Mono-substituted benzene (700 cm^{-1}) Si-OH (900 cm^{-1}) Aromatic C=C (1400-1750 cm^{-1}) C-H (2900-3100 cm^{-1}) O-H (3000-3600 cm^{-1}, broad)

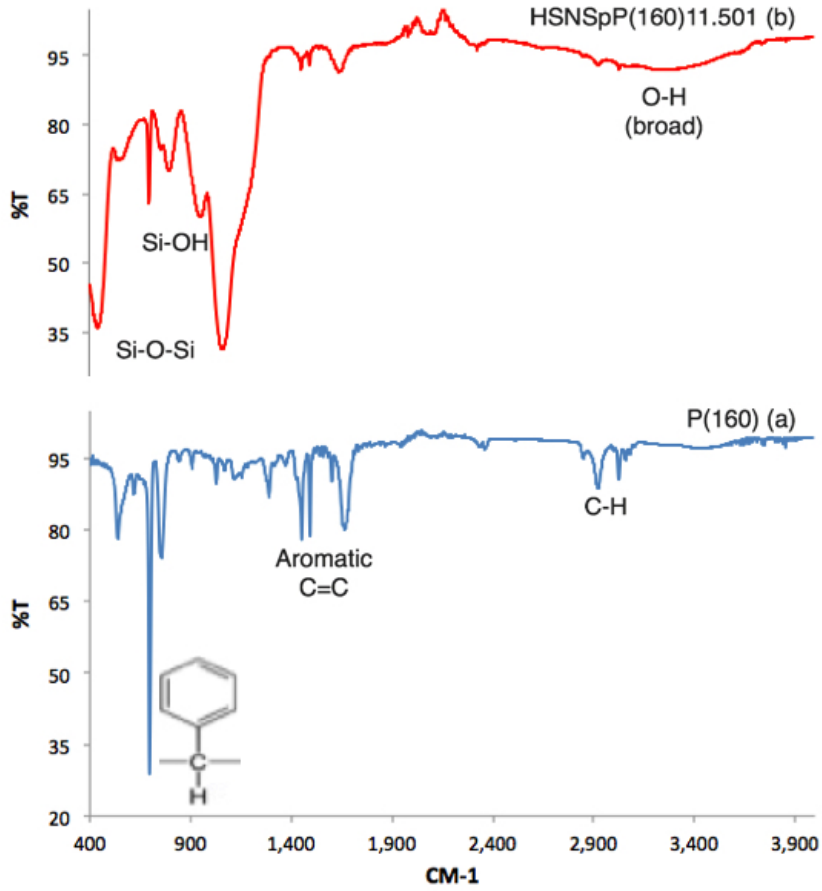

Figure 4.8: FTIR spectrum of the polystyrene nano - particles, P(160) (a) and the silica coated polystyrene sample, HSNSpP(160)11.501 (b).

Provided in Appendix C.2 are the FTIR spectra for all silica coated polystyrene samples in Figure C.10 and C.12. The composition change occurring during the preparation of the silica coated polystyrene sample HSNSpP(160) - 11.501, is a general occurrence for all silica coated polystyrene samples.

As - synthesised hollow silica nano spheres

The FTIR spectra of the silica coated polystyrene sample HSNSpP(160)11.501 and the as - synthesised HSNS sample HSNSP(160)11.501 are displayed in Figure 4.9. As mentioned previously, the FTIR spectrum of HSNSpP(160)11.501 shows the characteristic polystyrene IR bands along with $Si-O-Si$ bonds, $Si-OH$ bonds and $H-O$ bonds . For the FTIR spectrum of HSNSP(160)11.501, only the presence of $Si-O-Si$ bonds can be identified. This provides a strong indication that the polystyrene has been completely removed during heat treatment along with the hydroxide groups attached to the silica surface. The removal of polystyrene along with hydroxide groups is a general occurrence for all as - synthesised HSNS.

Table 4.6 lists the functional groups identified for four as - synthesised HSNS samples along with the weight and mass change (ΔM (%)) of the samples before and after heat treatment. Provided in Appendix C are all the FTIR spectra of as - synthesised HSNS samples in Figure C.11 and C.13, including HSNSP(160)11.461, HSNSP(160)11.491 and HSNSP(160)11.902.

Table 4.6: Main components identified and weight before and after heat treatment for the four as - synthesised HSNS samples: HSNSP(160)11.461, HSNSP(160)11.491, HSNSP(160)11.501 and HSNSP(160)11.902.

Sample:	Groups identified: (FTIR)	Before (g)	After (g)	ΔM (%)
HSNSP(160)11.461	Si-O-Si (450, 800, 1100 cm^{-1})	2.316	1.125	-51.4
HSNSP(160)11.491	Si-O-Si (450, 800, 1100 cm^{-1})	6.838	1.879	-72.3
HSNSP(160)11.501	Si-O-Si (450, 800, 1100 cm^{-1})	2.281	1.470	-35.6
HSNSP(160)11.902	Si-O-Si (450, 800, 1100 cm^{-1})	2.391	1.448	-39.4

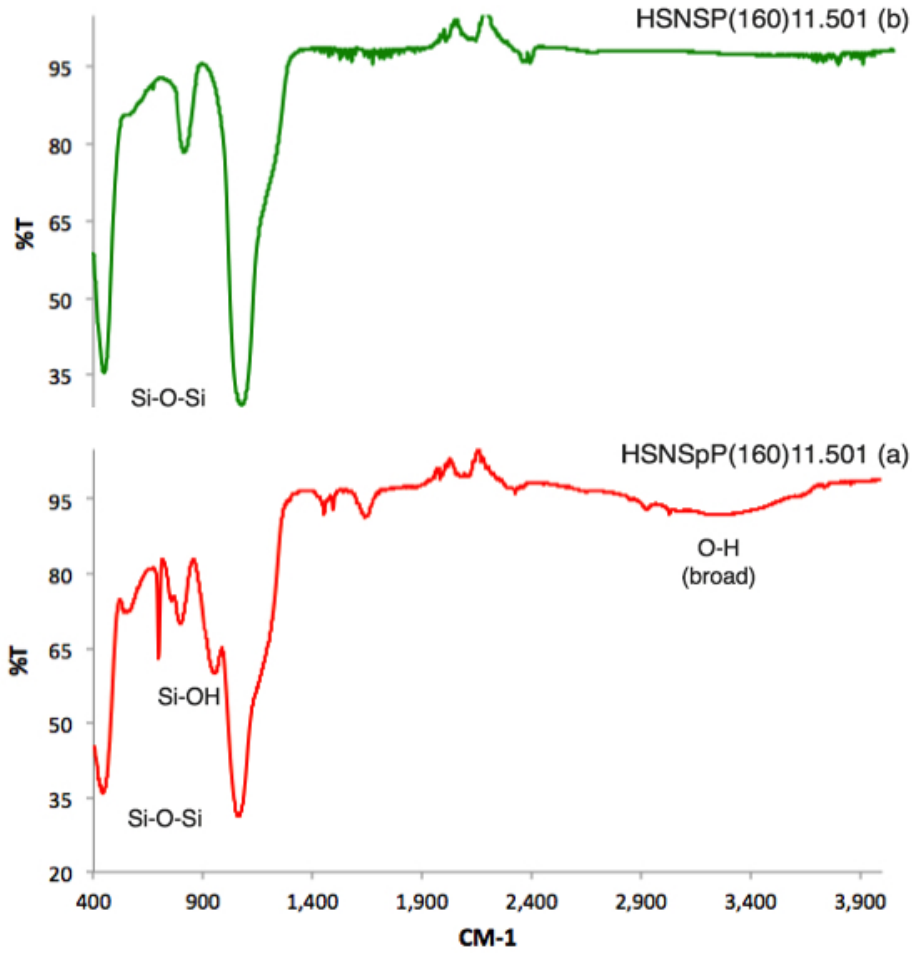

Figure 4.9: FTIR spectrum of the HSNS samples: HSNSpP(160)11.501 (a) and HSNSP(160)11.501 (b).

Hydroxylated hollow silica nano spheres

The hydroxide groups are to a large extent removed from the silica surface during the heat treatment. The FTIR spectra shown in Figure 4.10 represent the silica coated polystyrene sample HSNSpP(160)11.501 (a), the as - synthesised sample HSNSP(160)11.501 (b) and the hydroxylated sample, HSNShP(160)11.501 (c). $H-O$ bonds have a dominating vibration between 2900 and 3600 cm^{-1} and therefore the effectiveness of the hydroxylation process are determined in this region.

In the silica coated polystyrene sample the hydroxide groups are highly noticeable. However, for the as - synthesised HSNS sample the hydroxide groups have been removed to such an extent that it is not possible to confirm their presence from the spectrum. The hydroxylated sample has gained a moderate amount of hydroxide groups during the surface modification with respect to the broad band on HSNShP(160)11.501 compared to HSNSP(160)11.501. The addition of hydroxide groups on the silica surface during hydroxylation is a general occurrence for all hydroxylated HSNS samples. The only deviations are cases where as - synthesised HSNS samples exhibit a hydrophobic property instead of a hydrophilic property. This phenomenon is described more in detail in section 4.2.3.

Table 4.7 lists the extent of presence of hydroxide groups for five HSNS samples. Provided in Appendix C are all the FTIR spectra of hydroxylated HSNS in Figure C.14 and C.15.

Table 4.7: Presence of hydroxide groups in the HSNS samples HSNSpP(160)11.501, HSNSP(160)11.501, HSNShP(160)11.501, HSNShP(160)11.901 and HSNShP(160)11.902, , due to FTIR investigations.

Sample:	Presence of hydroxide molecules:
HSNSpP(160)11.501	Large extent
HSNSP(160)11.501	Un - identifiable
HSNShP(160)11.501	Moderate extent
HSNShP(160)11.901	Moderate extent
HSNShP(160)11.902	Un-identifiable

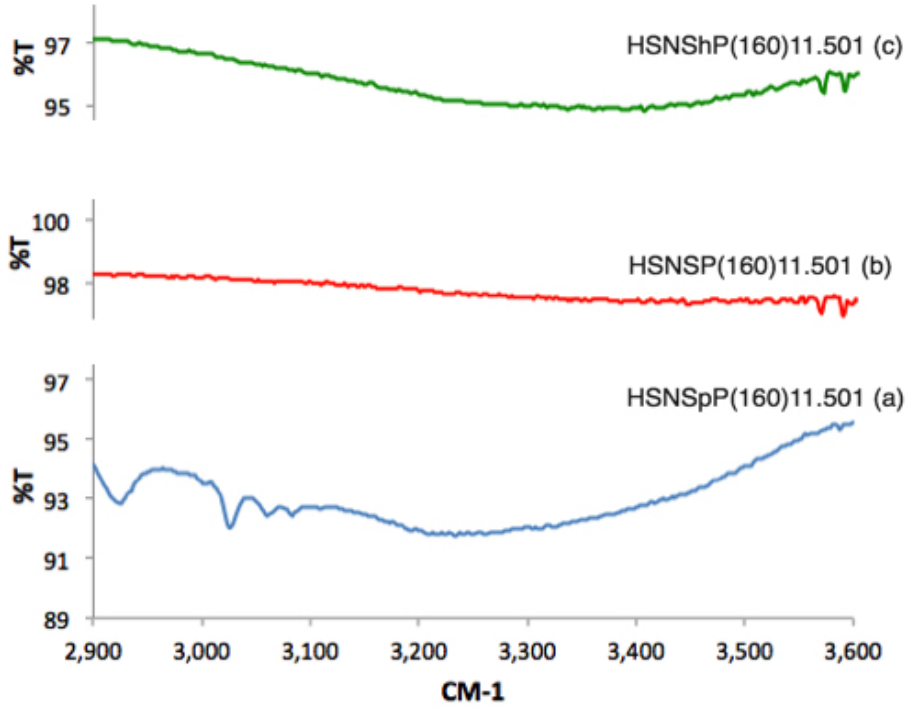

Figure 4.10: FTIR spectra of the HSNS samples: HSNSpP(160)11.501 (a), HSNSP(160)11.501 (b) and HSNShP(160)11.501 (c). Notice that the FTIR spectra are only displayed in for wavelengths between 2900 and 3600 cm^{-1}.

Functionalised hollow silica nano spheres

The FTIR spectra of the hydroxylated sample, HSNShP(160)11.551 (a) and the functionalised HSNS sample, HSNSfP(160)11.551 (b) are shown in the wavelength region 400 - 2000 cm^{-1}, in Figure 4.11. The hydroxylated HSNS sample, HSNShP(160)11.551 (a) only contains the three characteristic bands for $Si-O-Si$ bonds in this wavelength region. The FTIR spectrum of the functionalised HSNS sample, HSNSfP(160)11.551 provides a strong indication that the VMOS molecules (Figure 2.19) have successfully been attached to the surface of the silica. Based on the small amount of VMOS compared to the bulk of the material, the FTIR spectra of all the functionalised HSNS samples only contains bands with a low intensity, but large enough to confirm their presence.

At 950 cm^{-1} the presence of $C=C-H_2$ is identifiable. Additionally two smaller bands at 1400 cm^{-1} and 1580 cm^{-1} confirms the presence of $C-H$ bonds and $C=C$ bonds, respectively. Table 4.8 lists the functional groups identified for the functionalised HSNS sample HSNSf - P(160)11.551. After functionalisation all functionalised HSNS samples contained the bands previously described. Hence the attachment of carbon double bonds was successful on the silica surface, providing possibilities for further modification.

Provided in Appendix C are FTIR spectra of all functionalised HSNS samples in Figure C.16.

Table 4.8: Functional identified of the functionalised HSNS sample HSNSfP(160)11.551.

Sample:	Functional groups identified (FTIR):
HSNSfP(160)11.551	Si-O-Si (450, 800, 1100 cm^{-1}) C=C-H_2 (950 cm^{-1}) C-H (1400 cm^{-1}) C=C (1580 cm^{-1})

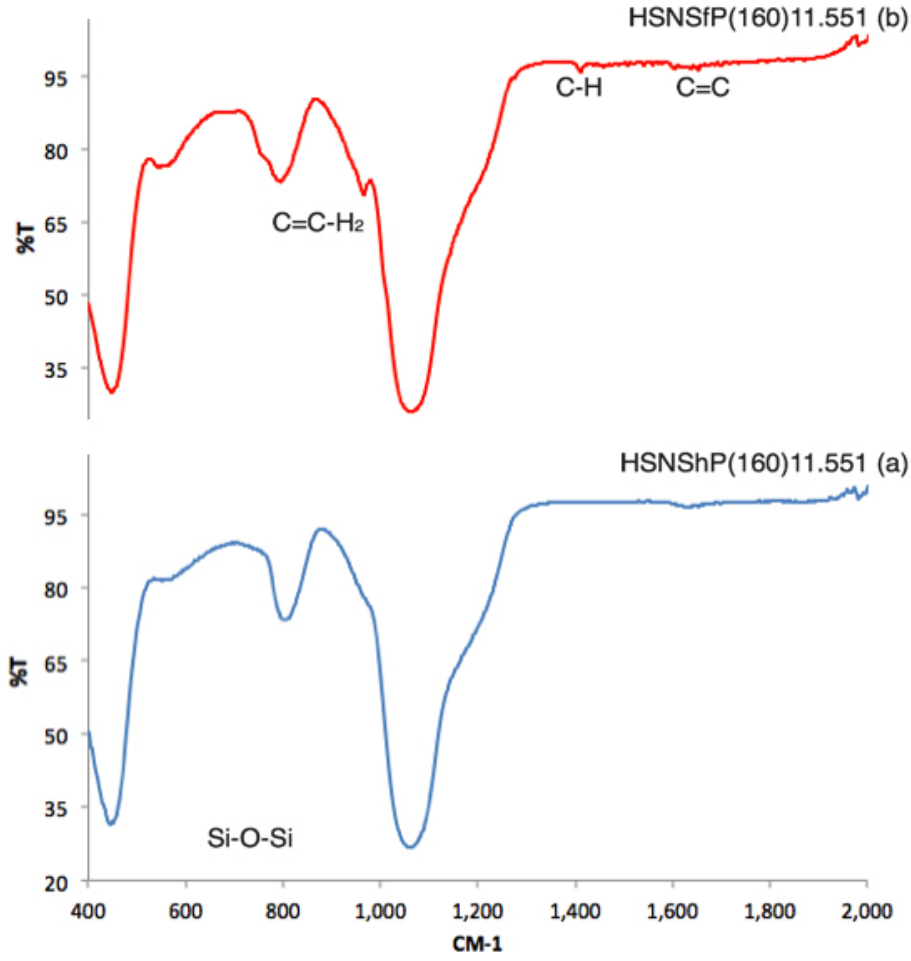

Figure 4.11: FTIR spectra of the HSNS samples: HSNShP(160)11.551 (a) and HSNSfP(160)11.551 (b).

4.2.3 Hydrophobicity

Silica coated polystyrene, as - synthesised and hydroxylated HSNS

90 % of all silica coated polystyrene, as - synthesised and hydroxylated HSNS samples prepared, generated hydrophilic (high wettability) properties. Only samples with a morphology of agglomerated spheres and a film of silica did in some rare cases generate hydrophobic (low wettability) properties. Table 4.9 lists the samples that exhibit hydrophobic properties before functionalisation.

The cases where hydrophobic properties occurred after the coating process were analysed to determine the deviations leading to this phenomenon. The HSNS sample HSNSP(140)11.902 which exhibited hydrophobic properties directly after the coating, was studied in detail along with its parallel: HSNSP(140) - 11.901, exhibiting hydrophilic properties after coating. The synthesis parameters and heating profile for the preparation of these two samples are identical, with only a slight difference in addition of ammonia - solution (Δ 0.3 ml, Table 3.2).

The SEM micrographs shown in Figure 4.12 illustrate the morphology of the as - synthesised HSNS samples, HSNSP(160)11.901 (a) and HSNSP(160)11.902 (b). Both samples are highly agglomerated producing spheres with an average diameter above 600 nm. The samples also exhibit a film of silica and multiple holes on each agglomerated sphere. Hence, the samples have an almost identical morphology which should promote a similar hydrophobicity. The FTIR spectra shown in Figure 4.13 were analysed to determine if contaminants were introduced to the samples during the synthesis. But in comparison the two FTIR spectra are identical.

Table 4.9: HSNS samples exhibiting hydrophobic properties before functionalisation.

Sample:	Morphology:	Heat treated:	Hydroxylated:
HSNSP(160)11.702	Agglomerated spheres 500 nm diameter	Hydrophobic	Hydrophobic Un-reactive
HSNSP(160)11.902	Agglomerated spheres 620 nm diameter	Hydrophobic	Hydrophobic Un-reactive

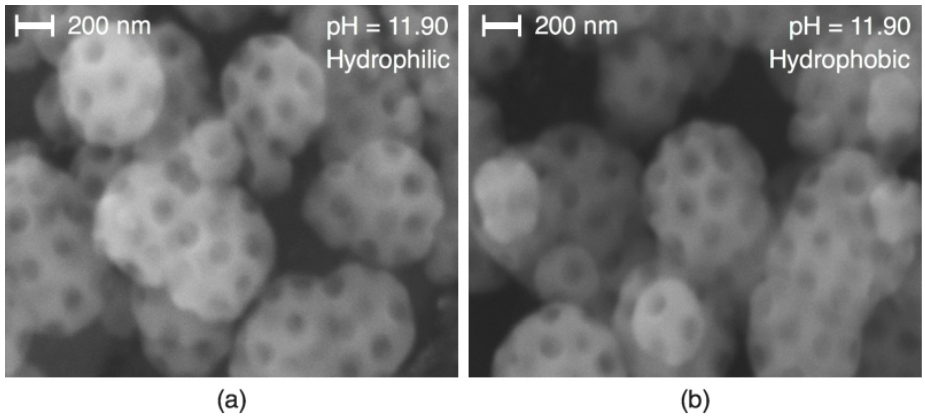

Figure 4.12: SEM micrographs of the as - synthesised HSNS samples: HSNSP(160)11.901 (a) and HSNSP(160)11.902 (b).

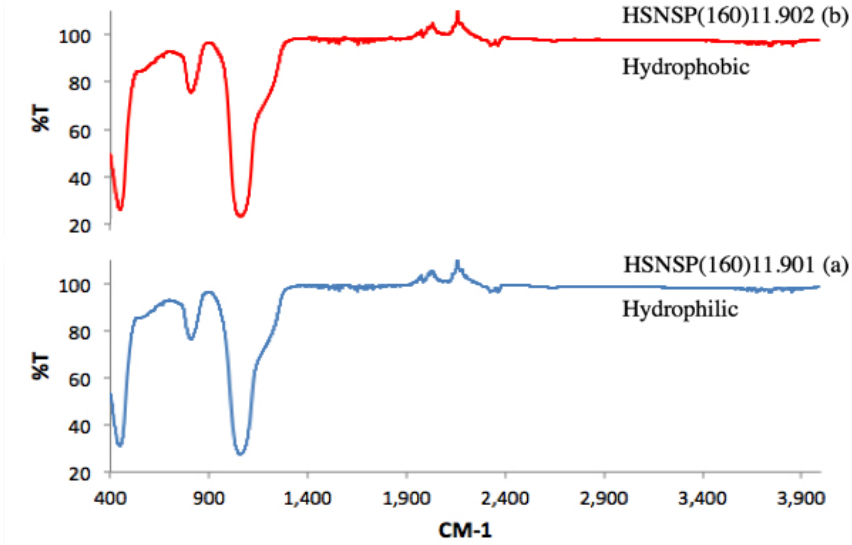

Figure 4.13: FTIR spectra of the as - synthesised HSNS samples: HSNSP(160)11.901 (a) and HSNSP(160)11.902 (b).

Hydrophobisated hollow silica nano spheres

All HSNS samples which were hydrophobisated did not exhibit any change in hydrophobicity, morphology or composition compared to their precursors. Figure 4.14 and Figure 4.15 illustrate SEM micrographs and FTIR spectra, respectively, of the modified HSNS sample HSNShfP(140)12.002 (a) and its precursor HSNShP(140)12.002 (b). Both the morphology from the SEM micrographs and the composition from the FTIR spectra, indicate that the organic groups from HMDS molecule, has not been successfully attached to the surface.

Figure 4.16 illustrates the deposition of water on the surface of the hydrophobisated HSNS sample, HSNShP(140)12.002. Based on small yields during the hydrophobisation process, a sufficiently large pellet for contact angle measurements was not achievable. However, based on the formation of a water layer on the surface in Figure 4.16, the hydrophobisation process did not altered the hydrophobicity of HSNS material. The formation of a water layer was a general occurrences for all hydrophobisated samples.

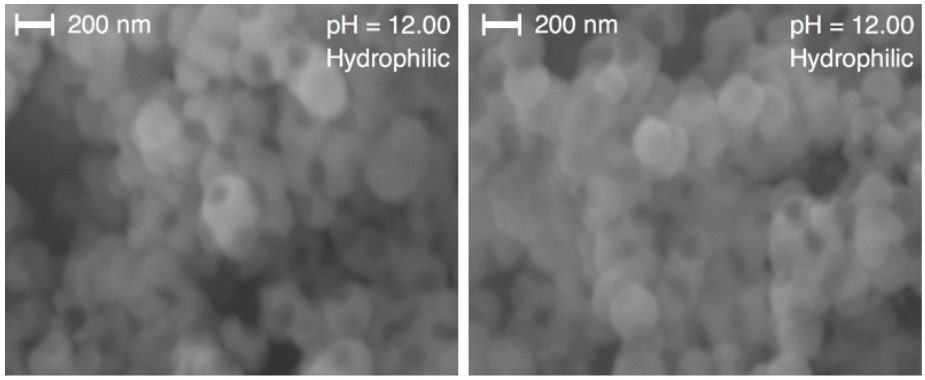

Figure 4.14: SEM micrographs of the modified HSNS sample HSNShfP(140)12.002 (a) and its precursor HSNShP(140)12.002 (b).

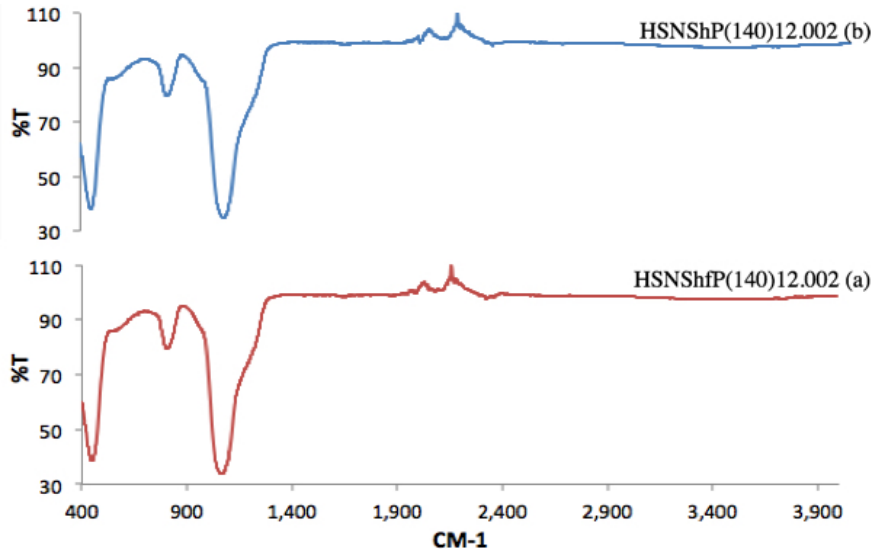

Figure 4.15: FTIR spectra of the modified HSNS sample HSNShfP(140)12.002 (a) and its precursor HSNShP(140)12.002 (b).

Figure 4.16: Observation image of the hydrophilic properties of the hydrophobisated HSNS sample, HSNShfP(140)12.002.

Functionalised hollow silica nano spheres

All functionalised HSNS samples prepared, produced materials with super hydrophobic properties. Table 4.10 lists the morphology along with the hydrophobicity after functionalisation of five HSNS samples. Figure 4.17 illustrates contact angle measurements done on the hydroxylated HSNS sample HSNShP(160) - 11.551 and the functionalised HSNS sample HSNSfP(160)11.551. The hydroxylated HSNS sample interacted with the water droplet generating a wet layer on the surface. The wet layer produced during the contact angle measurement is a general occurrence for a super hydrophilic (complete wetting) material and provides a contact angle equal to zero on the interface between the solid surface and the water droplet. After functionalisation the HSNS sample's hydrophobicity was significantly altered. In Figure 4.17, (b), the blue line represents the baseline (the interface between the solid material and the water droplet), the red line is the curvature of the droplet and the two green angles is the contact angle based on the baseline. The baseline, curvature and angles were generated from the analysing program of DSA 1000. The contact angle measured for the functionalised HSNS sample HSNSfP(160)11.551 (b) was 153.5 °.
Hence a drastic alteration compared to the hydroxylated HSNS sample occurred. The functionalised HSNS samples became a super hydrophobic (non - wetting) material with a contact angle > 150 °.

Table 4.10: Morphology and hydrophobicity after functionalisation of five HSNS samples.

Sample:	Morphology:	Functionalisation:
HSNSfP(160)11.401	Porous silica coating (40 nm) 220 nm diameter	Super hydrophobic
HSNSfP(160)11.461	Film silica (30 nm) 190 nm diameter	Super hydrophobic (Contact angle)
HSNSfP(160)11.501	Porous silica coating (30 nm) 200 nm diameter	Super hydrophobic
HSNSfP(160)11.551	Film silica coating (40 nm) 210 nm diameter	Super hydrophobic (Contact angle)
HSNSfP(160)11.651	Film silica, moderate ag 400 nm diameter	Super hydrophobic
HSNSfP(160)11.761	Film silica, high ag 500 nm diameter	Super hydrophobic (Contact angle)

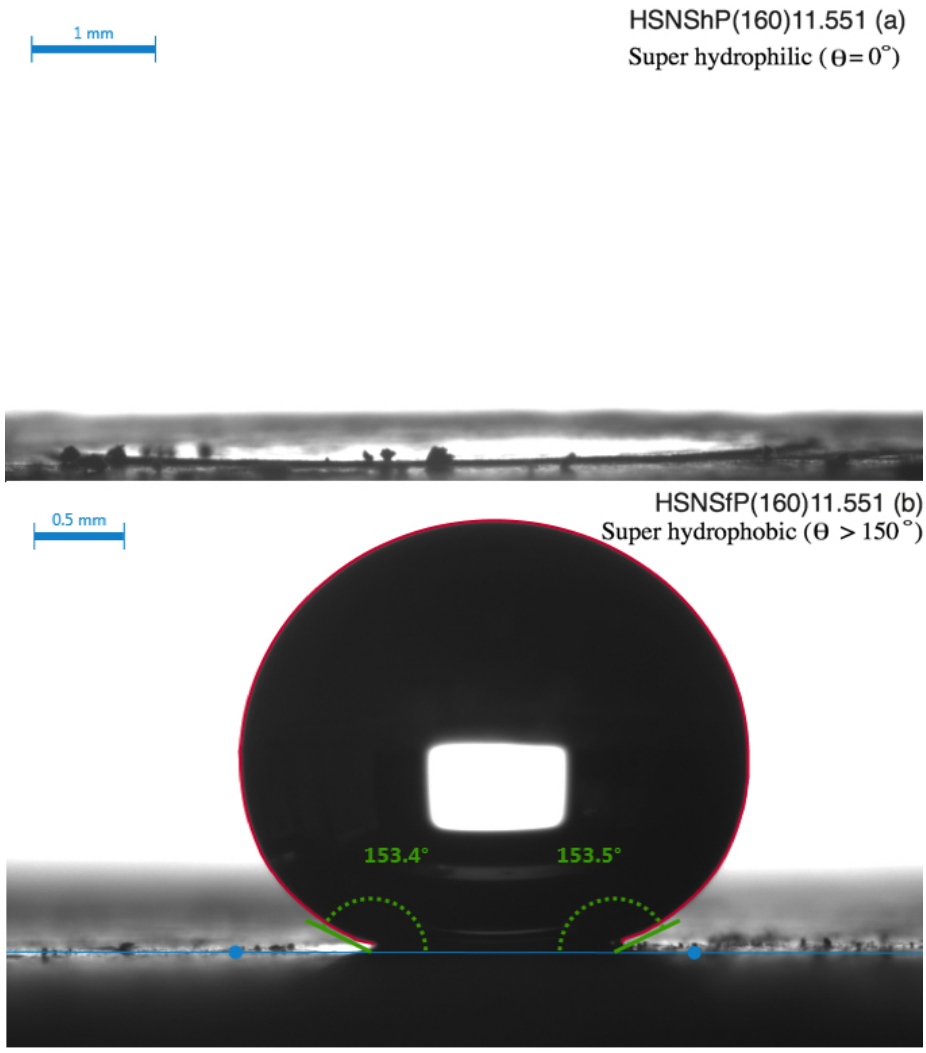

Figure 4.17: Contact angle measurement of the HSNS samples, HSNShP(160)11.551 (a) (super hydrophilic) and HSNSfP(160)11.551 (b) (super hydrophobic). Notice the difference in magnification between (a) and (b).

Figure 4.18 illustrates six additional contact angle measurements for the functionalised HSNS samples, HSNSfP(160)11.461 and HSNSfP(160)11.761. Where (a), (c) and (e) are parallel measurements done at different positions on the surface of HSNSfP(160)11.461 and (b), (d) and (f), respectively, on HSNSfP(160)11.761. All contact measurements done on functionalised HSNS samples produced a contact angle > 150 °.

4.2.4 Thermal conductivity

The thermal conductivities of the as - synthesised sample, HSNSP(160)11.491 and the functionalised sample, HSNSfP(160)11.461 were measured and are represented by the two equations (4.1) and (4.2):

$$\kappa_{HSNS(P160)11.491} = 0.0651 \pm 0.005 \quad [mWm^{-1}K^{-1}] \tag{4.1}$$

$$\kappa_{HSNSfP(160)11.461} = 0.0643 \pm 0.005 \quad [mWm^{-1}K^{-1}] \tag{4.2}$$

The thermal conductivity measured for the two HSNS materials is high with respect to super insulating materials (SIM) (> 25 $(Wm^{-1}K^{-1})$. Table 4.11 lists the morphology and hydrophobicity of the two HSNS materials.

Based on the structure of the samples, the large thermal conductivity is reasonable. The hollow inside has a diameter similar to the polystyrene templates used during preparation (≈ 160 nm). The mean free path of air at regular conditions is significantly smaller than the pore diameter for both the HSNS materials. Hence gas - gas collisions will be dominating and self - diffusion occurs rather than the wanted Knudsen diffusion. The silica surface of both HSNS materials exhibit a film of silica rather than the wanted coverage of silica nano particles. and the pellet produced for the thermal conductivity measurements, varies in density along with containing possible air holes.

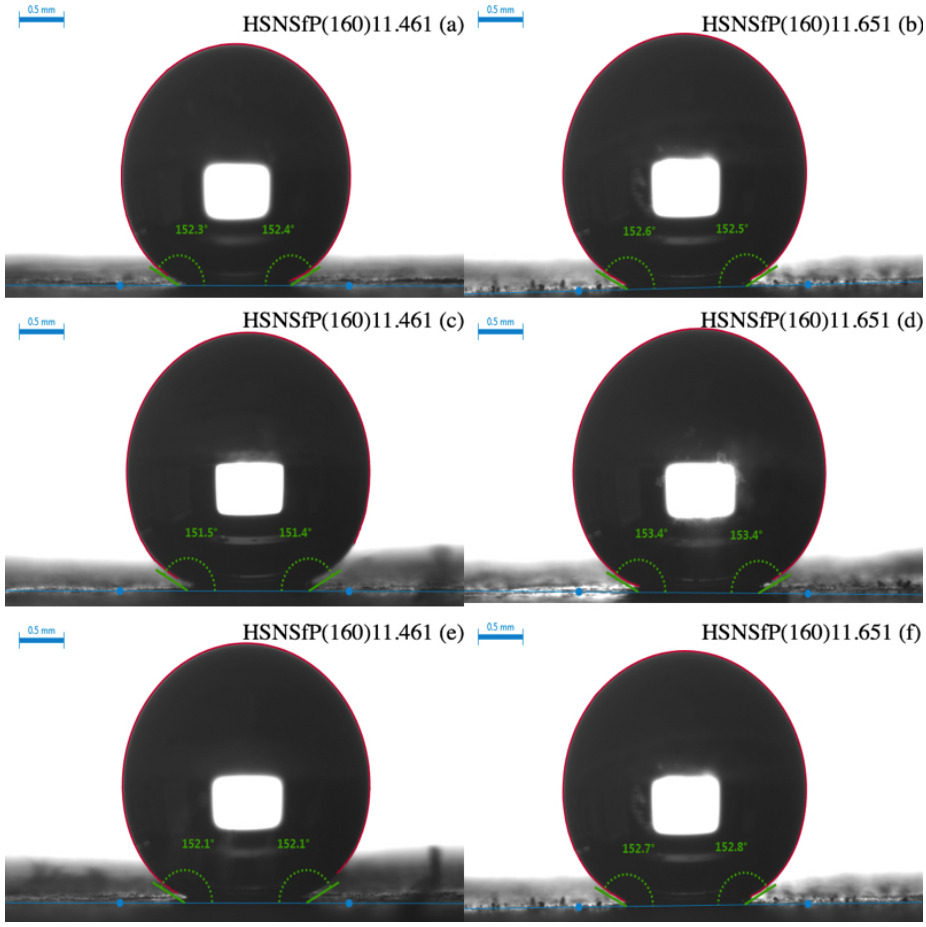

Figure 4.18: Contact angle measurement of the functionalised HSNS samples: HSNShP(160)11.461 and HSNSfP(160)11.651. (a), (c) and (e) are parallel measurements done on HSNSfP(160)11.461 at different locations on the surface, while (b), (d) and (f) are parallel measurements done on HSNSfP(160)11.651 at different locations on the surface.

When comparing the thermal conductivity of the two materials, there is only a slight difference ($\Delta \pm 0.0008$ $[mWm^{-1}K^{-1}]$) between them and the uncertainty of the measurement ($\Delta \pm 0.005$ $[mWm^{-1}K^{-1}]$) is significantly higher than than the difference between them. With respect to the uncertainty, the difference between thermal conductivity of the functionalised HSNS material compared to the heat treated HSNS material is negligible.

Summarised, the functionalised material has produced a super hydrophobic surface, along with possibilities for further modifications without altering the thermal conductivity.

Table 4.11: Morphology and hydrophobicity of the two HSNS samples, HSNSP(160)11.491 and HSNSfP(160)11.461.

Sample:	Morphology:	Hydrophobicity:
HSNSP(160)11.491	Film silica coating (30 nm) 200 nm sphere diameter	Super hydrophilic
HSNSfP(160)11.461	Film silica coating (30 nm) 200 nm sphere diameter	Super hydrophobic

Chapter 5

Discussion

5.1 Polystyrene

During further preparation of HSNS, the polystyrene templates are in a solution containing contaminants such as water. The polystyrene SEM micrographs (Figure 4.1) and FTIR spectra (Figure 4.2) were measured after air drying the polystyrene templates. Provided in Appendix C are a FTIR measurement of the polystyrene batch P(140) in solution in Figure C.9.

The experimental procedure based on Sandberg et al. [24], is a simple synthesis method producing polystyrene templates with a average diameter between 120 and 200 nm. On all successful polystyrene batches synthesised (Appendix B, Table B.2), the sphere diameter varied by less than 15 nm. In order to obtain Knudsen diffusion the nano - spherical polystyrene templates need to exhibit a diameter below the mean free path of air (64 nm at regular conditions). Preferably a diameter between 20 to 40 nm would generate a dominating Knudsen diffusion, based on the increase in probability for a gas - pore wall collision occurring, compared to a gas - gas collision. The surfactant (PVP) used during polymerisation, is not able to generate enough surface tension to produce polystyrene with a diameter below 100 nm. The polystyrene templates are removed during heat treatment and based on the chemical components of polystyrene, both producing and burning this material away is not environmentally friendly. Hence the synthesis method needs to be modified or replaced with an alternative method such as a Sol - gel process [39].

Based on the simplicity of the experimental procedure and the uniformity produced, the method is acceptable for a low scale production to analyse the properties. In a large scale production both large diameter and the environmental impact polystyrene causes would not produce the wanted commercial product.

5.2 Hollow Silica nano spheres

Low concentration of ammonia (low pH)

The unwanted morphology produced by the addition of ammonia solution > 1.5 mL, was further investigated to characterise the occurrence. The low concentration of ammonia results in a low rate of hydrolysation (Figure 2.12). One theory concerning the generation of blocks is that the coating duration (24 h) with a low ammonia concentration is not long enough to properly initiate the hydrolysation reaction. After centrifugation, the silica coated polystyrene are air - dried. During this period the main reaction occurred with the small amount of remaining liquid. This forms a silica - polystyrene network rather than seperate polystyrene spheres coated with silica. A second theory is that a lack of hydrolysed TEOS molecules, promotes attachment of the polystyrene spheres with each other, also leading to a formation of a silica - polystyrene network.

The heat treatment of the HSNS samples, HSNSpP(110)11.301 (Figure 4.3, (a)) and HSNSpP(110)11.301 (Figure 4.3, (b)) promotes these theories based on the significant alteration occurring, compared to HSNS samples synthesised with a higher concentration of ammonia. After heat treatment the samples do not exhibit the same white colour as before. However, a brownish colour characteristic for an incomplete decomposition of carbon is generated.

Acidic catalyst

With the use of an acidic catalyst, hydrochloric acid (HCl) was attempted to produce HSNS similar to HSNS prepared with a basic catalyst. Four preparations were attempted and each synthesis resulted in a extremely low yield along with unwanted structural generation. Table B.3 in Appendix B lists the experimental values of each synthesis.

All acid based preparations were significantly altered during the removal of polystyrene. Similar to basic catalysed HSNS samples with a low concentration of ammonia, the acidic catalysed HSNS samples generated a brown colour characteristic of the incomplete decomposition of carbon carbon. Based on the progression with the use of basic catalyst, further investigations of acidic catalysis and catalyst materials was not a priority.

Morphology generation with respect to basic catalyst

The credibility of the hypothesis, concerning the structural outcome of the hollow silica nano spheres with respect to the use of ammonia solution as a basic catalyst is still to be determined. Preparations of basic catalysed HSNS has only been done in the pH range from 11 to 12. Based on these preparations the amount of ammonia solution needed to achieve seperate spheres lies above 1.5 mL and producing spheres with no/slight agglomeration, required less than 5.5 $\pm$ 0.5 mL ammonia solution (Figure 4.4).

The initial ammonia solution had a concentration between 25 - 30 m% NH_3. The as - synthesised HSNS samples HSNSP(140)11.301 and HSNSP(140)11.302 were one of the first preparations, requiring an amount of 1.45 and 1.50 mL, respectively, of the ammonia solution to generate a pH of 11.30. HSNSP(160)11.303 and HSNSP(160)11.304 were done at a later point during this work, requiring 2.6 mL, to generate the same pH.

Assuming that the concentration of the ammonia solution was 25 m% during the preparation of HSNSP(140)11.301 the amount of NH_3 required to achieve a pH of 11.30 was calculated based on Equation 5.1:

$$p_{ammonia} \times m\%_{NH_3} \times V_{solution} = m_{NH_3} \tag{5.1}$$

Knowing the density of NH_3, the volume added and the concentration of NH_3 in the solution, the amount of ammonia added during coating of the HSNS sample, HSNSP(140)11.301 was calculated to:

$$m_{NH_3} = 0.8 \quad [gcm^{-3}] \times 0.25 \times 1.45 \quad [cm^3] = 0.29 \quad [g] \tag{5.2}$$

Based on the identical concentration parameters of HSNSP(140)11.301 and HSNSP(160)11.303, the amount of NH_3 corresponds directly to the pH of the

solution. Rearranging Equation 5.1 and assuming that an amount of 0.29 g of NH_3 corresponds to a pH of 11.30, the m% of NH_3 in the ammonia solution during the preparation of HSNSP(160)11.303 was calculated to:

$$\frac{0.29 \quad [g]}{0.8 \quad [gcm^{-3}] \times 2.6 \quad [cm^3]} = m\%_{NH_3} = 14\% \tag{5.3}$$

These calculations are approximations and 14 m% of NH_3 is the lower limit in the ammonia solution, when HSNSP(160)11.303 was synthesised. The addition of ammonia solution during the coating process provides a dilution of the basic catalyst, with respect to water from the polystyrene - solution, 96 % EtOH and the TEOS solution. Hence the ammonia solution is more concentrated than the calculations predict.

After preparation of HSNSP(160)11.303, additional seven HSNS samples were prepared, indicating a further decrease in concentration of NH_3 during coating on the very last HSNS samples. With respect to the calculations, the hypothesis of the morphology outcome based on the addition of ammonia solution is only valid for a concentration of NH_3 above 10 %. Ammonia solutions with a concentration of NH_3 below 10 % have not been used during this work and what effect a further decrease would promote is undetermined.

Hydrophobicity of as - synthesised HSNS samples

The two as - synthesised HSNS sample HSNSP(160)11.702 and HSNSP(160)11. - 902 exhibiting hydrophobic properties, consist of large agglomerated spheres with multiple holes. The increase in hydrophobicity only occurs in samples with a similar morphology. However, the generally hydrophobicity for HSNS samples produced with this morphology is hydrophilic. During heat treatment above 400 $°C$ silica becomes modified and based on the preparation method, all HSNS samples undergo this modification during the removal of polystyrene. The combination of agglomeration and modification of the silica surface might be the reason behind the generation of hydrophobic properties. The two HSNS samples HSNSP(160)11.901 and HSNSP(160)11.902 illustrated by SEM micrographs in Figure 4.12 have identical synthesis parameters and heating profiles, but HSNSP(160)11.901 exhibits hydrophilic properties while HSNSP(160)11.902 exhibits hydrophobic properties. Why this drastic difference in hydrophobicity occurs seems highly random and the phenomenon is not reproducible.

Hydrophobisation

The surface modification process hydrophobisation, did not alter the hydrophilic properties of silica coated polystyrene, as - synthesised and hydroxylated HSNS. The procedure has not been done previously on HSNS, but on the similar material, silica aerogels.

The structural properties between these materials are very similar, both consist of silica nano - particles with an extremely low density. On silica aerogels this surface modification was successful [30]. The reason why, the HSNS do not exhibit any morphology (Figure 4.14), composition (Figure 4.15) or hydrophobicity (Figure 4.16) change is uncertain. One possible explanation is the modification of silica occurring during the removal of polystyrene. The silica surface becomes less reactive compared to silica aerogels, but HMDS (Figure 2.16) is a highly reactive compound. The successful attachment of hydroxide groups during hydroxylation and attachment of $C = C$ bonds during functionalisation, provides a further uncertainty in regards to why the hydrophobisation process did not alter the silica surface. Hence the modification of silica during heat treatment is an unlikely explanation.

Determining the hydrophobicity

When determining the hydrophobicity of the functionalised HSNS samples using contact angle measurements the main issue was gravity. All functionalised samples exhibit super hydrophobic properties, indicating that the droplet deposited on the surface did not interact with the solid material. The pellet produced from the functionalised samples before the contact angle measurement does not exhibit an ideal surface. In both Figure 4.17 and 4.18 the surface on all measurements consists of small particles sticking out of the surface and in Figure 4.18 on HSNSfP(160)11.651, (b) and (f) the surface is slightly tilted.

When depositing the water droplet the main issue was that the droplet stays on the solid material. On all contact angle measurements a water droplet with the same volume was deposited on average, three times before it stayed on the material rather than rolling of, onto the sample carrier. The tendency for the water droplet to roll off is a clear indication that the interaction between the functionalised sample and water is weak. When further analysing the parallel measurements in Figure 4.18, the curvature generated from the analysing pro-

gram is not completely accurate. The occurrence can be noticed especially on HSNSfP(160)11.461 (c) and (e), where the curvatures on the lower right part of the water droplet are missing. For all contact angle measurements the measured contact angle is located slightly below the actual curvature. This error promotes that the contact angles measured, are lower than the actual contact angles between the interface, since the base - lines are in reality further upwards.

Figure 5.1 illustrates a contact angle measurement on HSNSfP(160)11.551, where the water droplet was deposited in the center of the surface and rolled until it stopped due to a cavity on the surface.

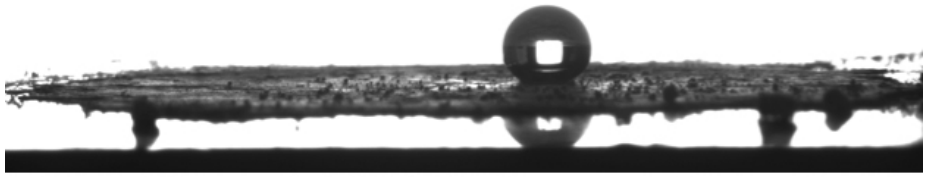

Figure 5.1: Contact angle measurement of the functionalised sample HSNSfP(160)11.551. Notice that the water droplet is not in the center of the solid material.

Chapter 6

Concluding remarks and future work

With the use of an ammonia solution varying between 10 - 30 m% NH_3, a structural outcome overview was accomplished. The morphology of the attached silica and the agglomeration of spheres was determined to be correlated with the addition of ammonia solution, rather than the pH of the coating solution. A porous silica coating with no agglomeration of spheres is the optimal morphology for insulation applications and Table 6.1 displays the relation between the amount of ammonia solution and the morphology of the attached silica, along with the agglomeration tendency of the spheres.

Table 6.1: Relation between the addition of ammonia solution and the morphology of the attached silica, along with agglomeration tendency of the spheres.

Amount of ammonia solution (10-30 m% NH_3) (mL)	Morphology	Agglomeration
$<1.5 \pm 0.5$	Silica - polystyrene network	Blocks
1.5 - 3.0 $\pm$ 0.5	Porous silica coating	None
3.0 - 5.5 $\pm$ 0.5	Film of silica	Slight
$>5.5 \pm 0.5$	Film of silica	High

The use of an acidic catalyst in all attempted preparations generated a silica - polystyrene network, rather than the wanted morphology of separate nano spheres.

The modification of the silica surface with the use of HMDS was attempted, to increase the hydrophobicity of the material. All modifications resulted in no variations in morphology, composition or hydrophobicity.

A surface modification process, functionalising the HSNS surface has been developed, producing a HSNS material with super hydrophobic properties ($\theta > 150°$) along with $C = C$ bonds attached to the surface. The components integrated during the functionalisation did not provide a negative impact on the thermal conductivity, compared the as - synthesised HSNS material.

The attached $C = C$ bonds provide promising possibilities for further research. With the use of a radical initiator or other polymerisation techniques, the $C = C$ bonds can be broken and attached to each other. Hence the connected spheres would exhibit a enhanced flexibility, reducing the brittleness of the material.

A radical initiator suitable could be, 2,2 - Azobis(2-methylpropionitrile) (ABIN) illustrated in Figure 6.1. The radicals generated by ABIN have the required energy to break the $C = C$ bonds and should not hinder the broken bonds to react with each other.

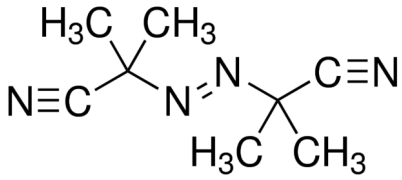

Figure 6.1: Chemical structure of the radical initiator 2,2 - Azobis(2-methylpropionitrile) (ABIN).

Lastly a modified method of template production or a different synthesis procedure, is essential to reduce the pore diameter below the average mean free path of air, along with reducing the negative environmental impact polystyrene causes. A Sol - gel process [39] would replace the solid template method, by a water - in - oil micro - emulsion. Hence the necessary heat treatment and the thereby occurring modification of the silica surface is removed. The sol - gel method has certain implications in regards to generating a uniform size distribution of the spheres throughout the material. This implication is the main reason why a solid template method (polystyrene) was used for preparing HSNS in this work. Without a uniform size distribution, analysing the HSNS materials with respect to the thermal conductivity and the morphology would be an issue.

Despite the use of a new template method for preparation of HSNS, the surface modification developed during this work is still applicable. The attachment of functional groups during functionalisation would not be affected by the use of a different template method.

Bibliography

[1] G. Slayter. Method and apparatus for making glass wool. 11 November 1933.

[2] D. Sen. Working with asbestos and the possible health risks. *Occupational Medicine*, 65(1):6–14, 2015.

[3] P. Webster. White dust black death: The tragedy of asbestos mining at baryulgil. *Trafford Publishing*, (9781412050777), 2006.

[4] Energy consumption in households. *Eurostat, Statistics Explained*, 2016.

[5] T. M. Tritt, editor. *Thermal conductivity: theory, properties and applications*. Number 0-306-48327-0. Kluwer Academic/ Plenum Publisheres, 2004.

[6] L. Wang. Generalized fourier law. *International Journal of Heat and Mass Transfer*, 37:2627–2634, November 1994.

[7] *Fundamentals of Heat and Mass transfer*. Number 978-0-470-50197-9. Wiley and sons, 7th edition, April 2011.

[8] I. Gnip et al. Thermal conductivity of expanded polystyrene (eps) at 10 °c and its conversion to temperatures within interval from 0 to 50 °c. *Energy and Buildings*, 52:107–111, 2012.

[9] J. Zach et al. Development of thermal insulating materials on natural base for thermal insulation systems. *Procedia Engineering*, 57:1288–1294, 2013.

[10] G. N. Li. Francis et al. Solid-wall u-values: heat flux measurements compared with standard assumptions. *Building Research & Information*, 43(2):238–252, 2015.

[11] R. Baetens et al. Aerogel insulation for building applications: A state-of-the-art review. *Energy and Buildings*, 43:761–769, 2011.

[12] T. Gao et al. Nano insulation materials: Synthesis and life cycle assessment. *Science Direct*, pages 490–495, 2014.

[13] M. Alam et.al. Vacuum insulation panels (vips) for building construction industry – a review of the contemporary developments and future directions. *Applied Energy*, 88(11):3592 – 3602, 2011.

[14] P. Solibakke. Synthesis of hollow silica nanospheres. Specialization project, Desember 2017.

[15] W.He et al. *Gas transport in Solid Oxide Fuel Cells, SpringerBriefs in Energy*. Number 2191-5520. Springer, 2014.

[16] S.G. Brush. *Kinetic Theory*. Number 9780080118703. Elsevier Ltd, January 1966.

[17] S.G Jennings. The mean free path in air. *Journal of Aerosol Science*, 19:159–166, 1988.

[18] K. Malek et al. Knudsen self- and fickian diffusion in rough nanoporous media. *The Journal of Chemical Physics*, 119:2800–2801, 2003.

[19] A. Berge et al. Literature review of high performance thermal insulation. *Building Physics*, 2012.

[20] M. Grandcolas et al. Hollow silica nanospheres as a superinsulating material. 09 2013.

[21] G.Solomons et al. *Organic chemistry*. Number 978-1-118-32379-3. Wiley and Sons, 2011.

[22] C.J. Brinker et al. *SOL-GEL SCIENCE*. Elsevier Inc, 1990.

[23] M. J. Rosen et al. *Surfactants and Interfacial Phenomena, 4th Edition*. Number 978-0-470-54194-4. WILEY, 2012.

[24] L. I. C. Sandberg et al. Synthesis of hollow silica nanospheres by sacrificial polystyrene templates for thermal insulation applications. *Advances in Materials Science and Engineering*, 2013:6, 2013.

[25] Sigma aldrich. Polyvinylpyrrolidone (pvp).

[26] Sigma aldrich. Tetraethyl orthosilicate (teos).

[27] M. Sletnes. Microstructural design of a silica thin lm for solar spectrum conversion layer using sol-gel synthesis. Master's thesis, NTNU, 2013.

[28] G.J Young. Interaction of water vapor with silica surfaces. *Journal of Colloid Science*, 13(1):67 – 85, 1958.

[29] A. Hoseini et. al. Effects of humidity on thermal preformance of aerogel insulation blankets. *Building Engineering*, 13:107–115, 2017.

[30] A. V. Rao et al. Effect of precursors, methylation agents and solvents on the physicochemical properties of silica aerogels prepared by atmospheric pressure drying method. *Journal of Non-Crystalline Solids*, 296:165–171, 2001.

[31] Sigma aldrich. Hexamethyldisiloxane (hmds).

[32] Sigma aldrich. Vinyltrimethoxysilane (vmos).

[33] Y. Liu et al. Accurate determination of the vapor-liquid-solid contact line tension and the viability of young equation. *Scientific Reports*, 3:2008 EP –, 06 2013.

[34] B. Krasovitski et al. Drops down the hill. theoretical study of limiting contact angles and the hysteresis range on a tilted plate. *Langmuir*, 21(9):3881–3885, 2005. PMID: 15835950.

[35] D. Zhao et al. Measurement techniques for thermal conductivity and interfacial thermal conductance of bulk and thin film materials. *Department of Mechanical Engineering, University of Colorado, Boulder*, (10.1115/1.4034605):19, October 2016.

[36] Thermtest. Characterizing the thermal conductivity of fuel cell diffusion media with the hot disk tps 2500s.

[37] Hitachi. Scanning electron microscope, flexsem 1000.

[38] Perkin Elmer. Identity verification and quality testing of polymers using mid infrared spectroscopy. *AZO materials*, 9 2015.

[39] Y. S. Lin et al. Synthesis of hollow silica nanospheres with a microemulsion as the template. *Chemical Communications*, 24(3):3542–3544, 2009.

[40] S. C. Feifel et al. Silica nanoparticles for the layer-by-layer assembly of fully electro-active cytochrome c multilayers. *Nano - biotechnology*, 9:59, 12 2011.

Appendix A

Reference spectra

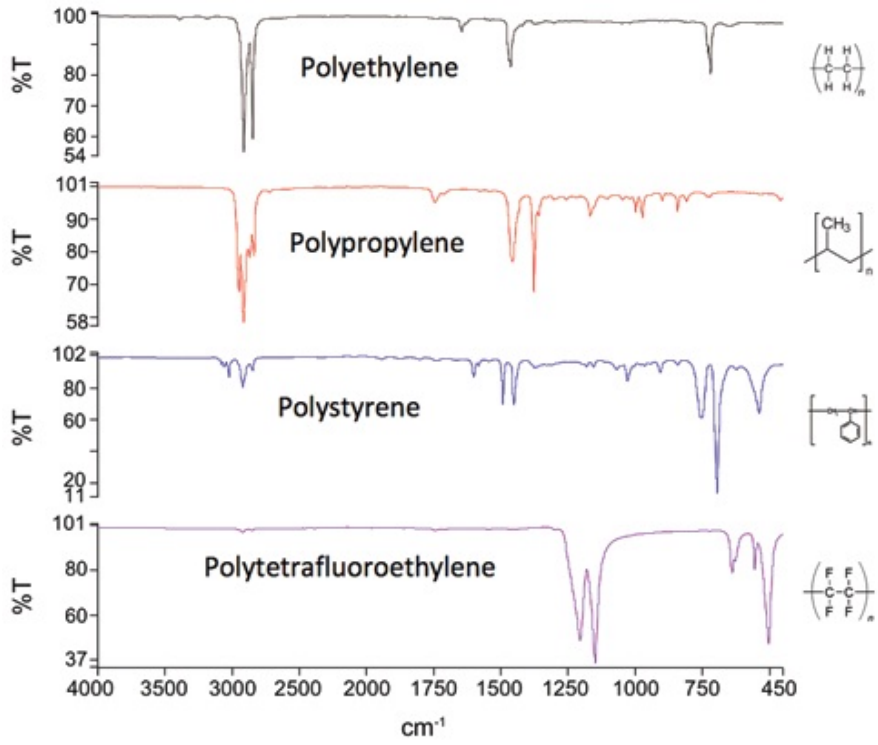

Figure A.1: FTIR reference spectrum of nano - particles of polystyrene, along with polyethylene, polypropylene and polytetrafluoroethylene[38]. Notice that the FTIR spectrum starts from a high wavelength.

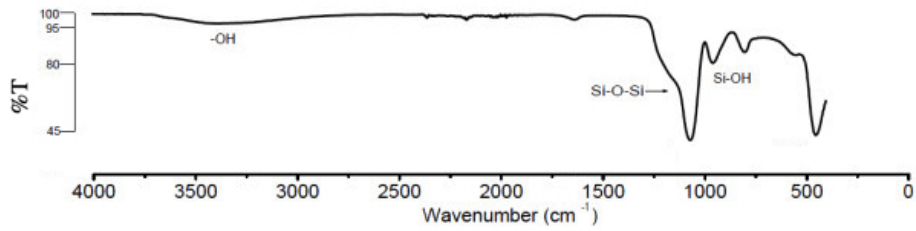

Figure A.2: Reference FTIR spectrum of silica nano - particles [40].

Appendix B

Additional experimental data

Table B.1: pH and the amount of basic/acidic catalyst in each coating synthesis.

Sample:	NH_4OH (mL)	pH
HSNSpP(160)11.191	3.35	11.19
HSNSpP(160)11.261	4.00	11.26
HSNSpP(140)11.301	1.45	11.30
HSNSpP(140)11.302	1.50	11.30
HSNSpP(160)11.303	2.6	11.30
HSNSpP(160)11.304	2.6	11.30
HSNSpP(160)11.401	2.5	11.40
HSNSpP(160)11.461	7.0	11.46
HSNSpP(160)11.491	6.0	11.49
HSNSpP(160)11.501	3.1	11.50
HSNSpP(160)11.502	3.5	11.50
HSNSpP(160)11.551	4.0	11.55
HSNSpP(200)11.601	9.8	11.60
HSNSpP(160)11.651	6.0	11.65
HSNSpP(160)11.701	4.7	11.70
HSNSpP(160)11.702	5.8	11.70
HSNSpP(160)11.761	8.0	11.76
HSNSpP(160)11.901	7.2	11.90
HSNSpP(160)11.902	7.5	11.92
HSNSpP(140)12.001	3.4	12.00
HSNSpP(140)12.002	3.4	12.00

Sample:	HCl (mL)	pH
HSNSpP(160)1.001	2.6	1.00
HSNSpP(160)1.002	2.6	0.99
HSNSpP(160)1.951	1.6	1.95
HSNSpP(160)2.001	1.5	2.00

Table B.2: Experimental values for the synthesis of nano -spherical polystyrene templates

No:	DW (g)	PVP (g)	Styrene (g)	KPS (g)	Stirring (rpm)	Container:	Temperature oil bath ($^{\circ}C$)
1	110.65	1.52	10.04	0.152 ± 0,005	None	Erlenmeyer	71
2	110.15	1.49	10.05	0.163 ± 0,005	500	Erlenmeyer	70
3	110.14	1.50	10.00	0.162 ± 0,005	500	Erlenmeyer	70
4	110.33	1.52	10.01	0.162 ± 0,005	500	Both	71
5	110.35	1.51	10.03	0.161 ± 0,005	500	Beaker	72
6	110.17	1.50	10.01	0.160 ± 0,005	500	Beaker	71
7	110.04	1.51	10.04	0.164 ± 0,005	500	Beaker	72
8	110.06	1.50	10.07	0.162 ± 0,005	500	Beaker	70

Table B.3: Experimental values for the coating synthesis of silica particles onto polystyrene templates with an acidic catalyst

No:	Polystyrene (g)	EtOH (mL)	TEOS-solution (mL)	HCl (mL)	pH	pH after TEOS
1	6.02	120	10	2.6	1.00	1.00
2	6.01	120	10	2.6	0.99	0.98
3	6.11	120	10	1.5	2.00	1.95
4	6.15	120	10	1.6	1.95	1.90

Appendix C

Additional results

SEM micrographs

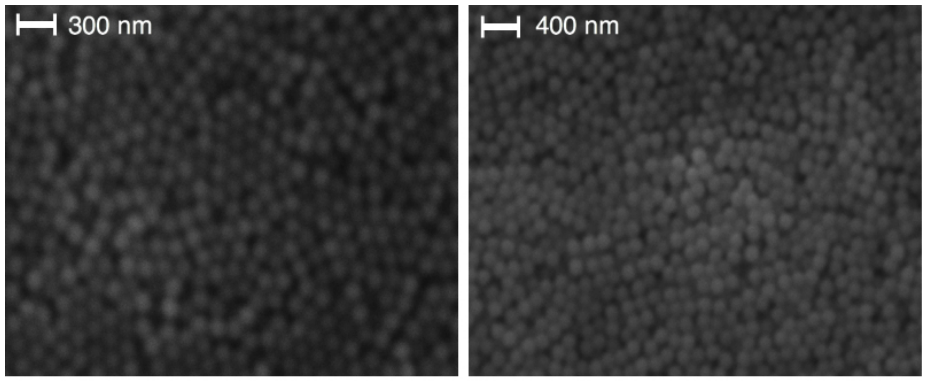

Figure C.1: Additional SEM micrographs of the polystyrene batches, P(140) and P(160). Notice the difference in magnification.

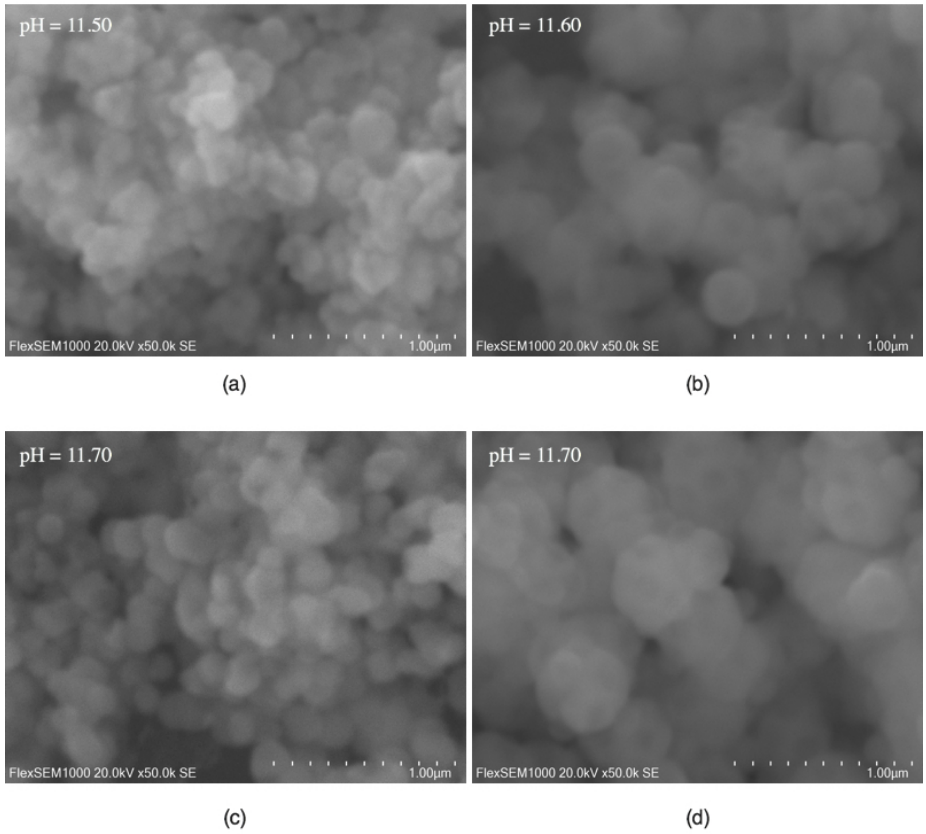

Figure C.2: SEM micrographs of the silica coated polystyrene samples, HSNSpP(160)11.502 (a), HSNSpP(200)11.601 (b), HSNSpP(160)11.701 (c) and HSNSpP(160)11.702 (d).

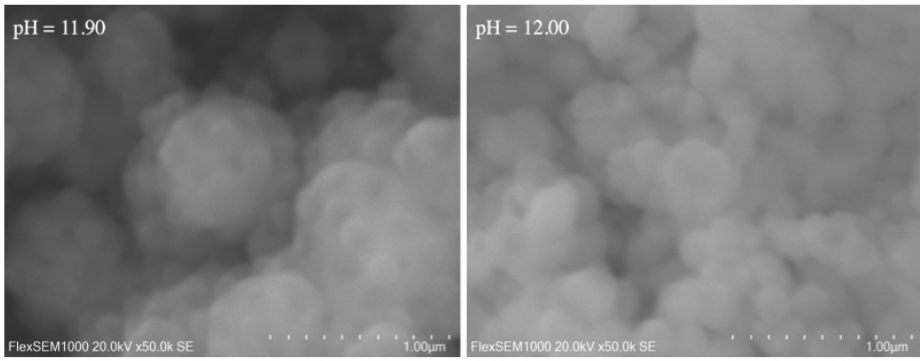

Figure C.3: SEM micrographs of the silica coated polystyrene samples, HSNSpP(160)11.902 (a) and HSNSpP(140)12.002 (b)

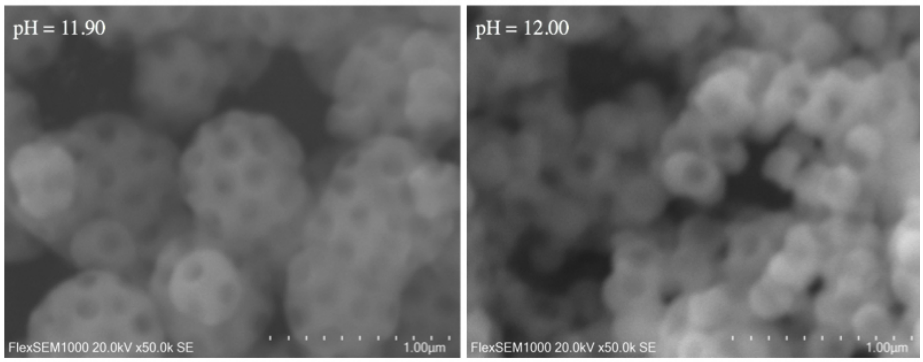

Figure C.4: SEM micrographs of the as - synthesised HSNS samples, HSNSP(160)11.902 (a) and HSNSP(140)12.002 (b).

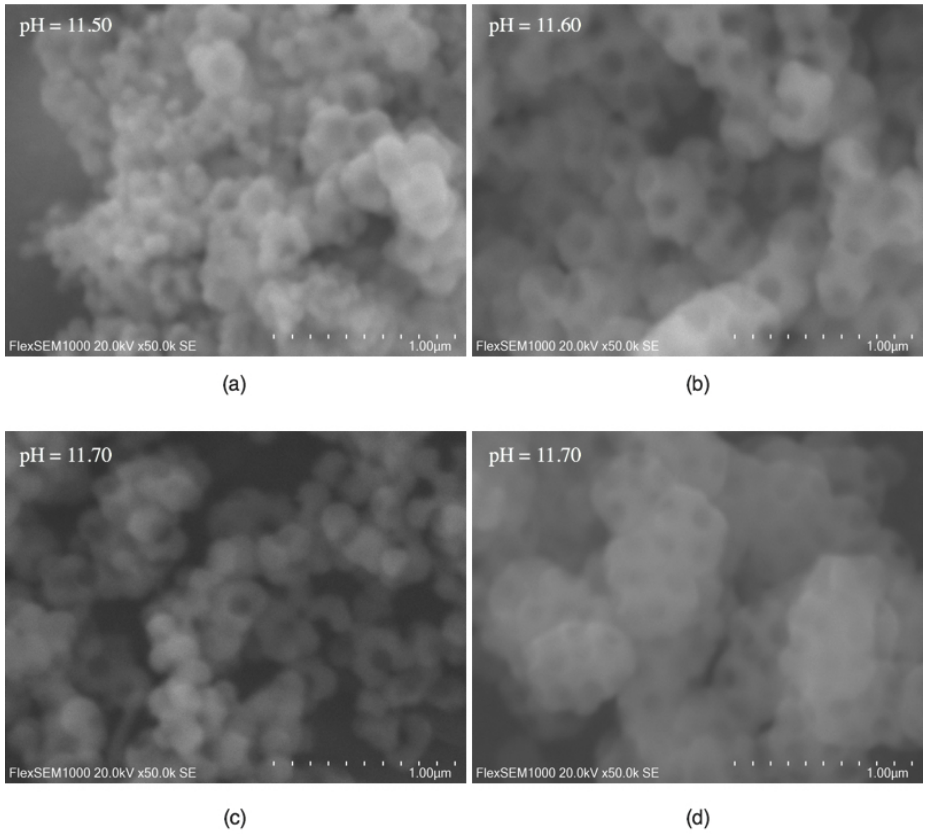

Figure C.5: SEM micrographs of the as - synthesised HSNS samples, HSNSP(160)11.502 (a), HSNSP(200)11.601 (b), HSNSP(160)11.701 (c) and HSNSP(160)11.702 (d).

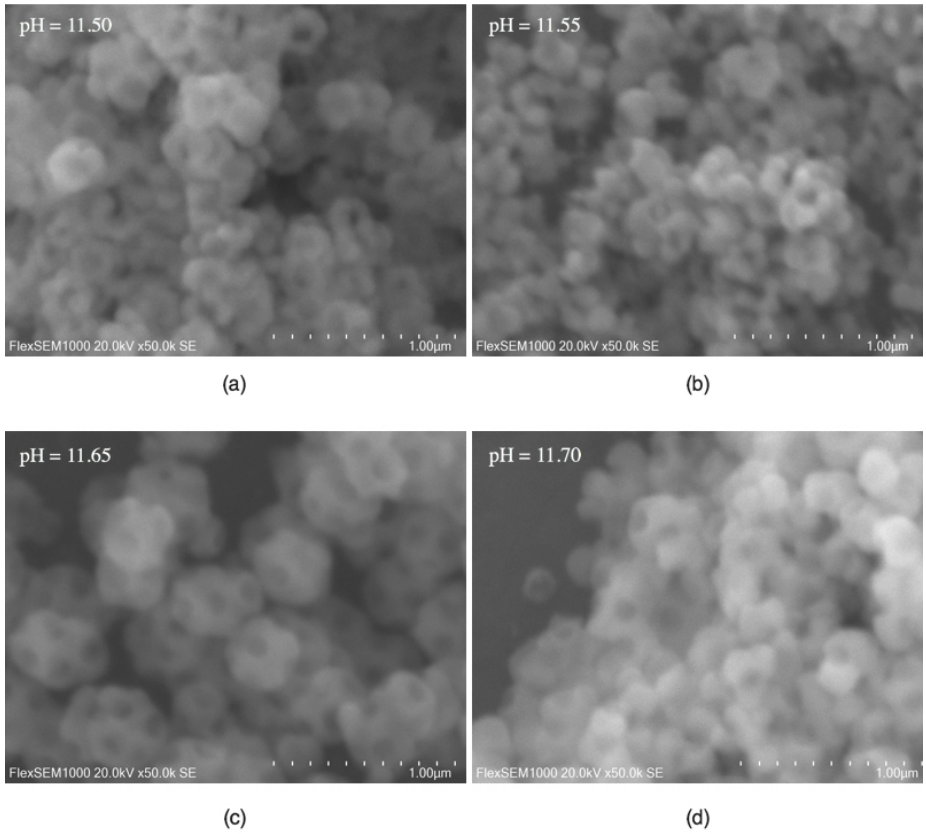

Figure C.6: SEM micrographs of the hydroxylated HSNS samples, HSNShP(160)11.502 (a), HSNShP(160)11.551 (b), HSNSP(160)11.651 (c) and HSNSP(160)11.701 (d).

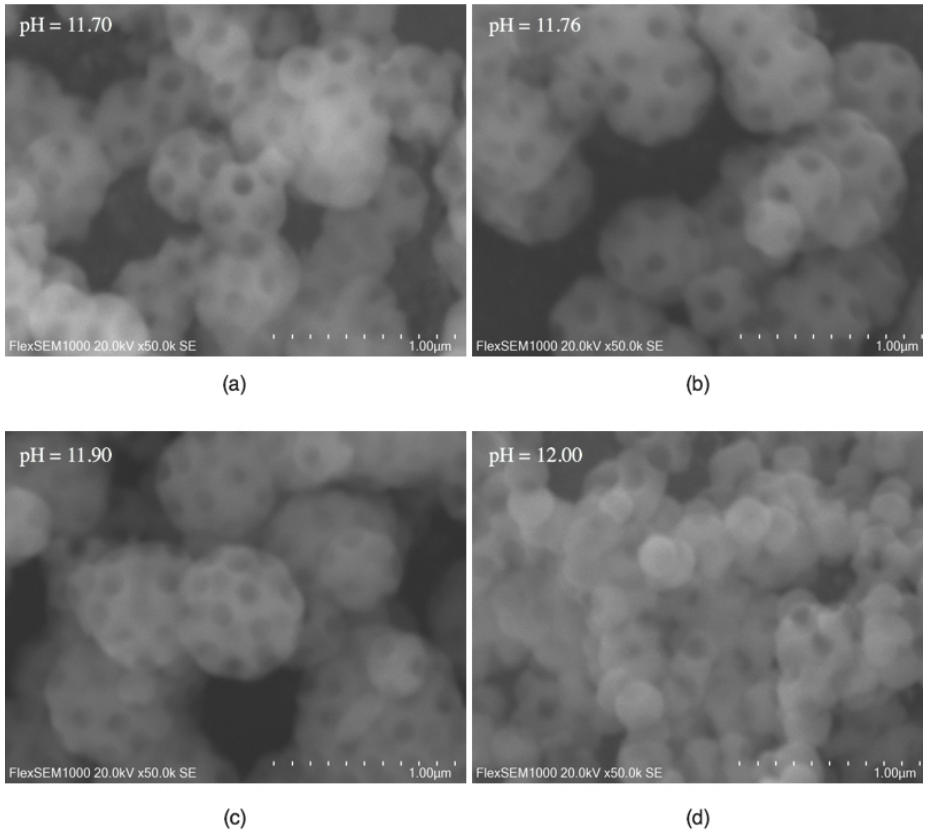

Figure C.7: SEM micrographs of the hydroxylated HSNS samples, HSNShP(160)11.702 (a), HSNShP(160)11.761 (b), HSNShP(160)11.902 (c) and HSNShP(140)12.002 (d)

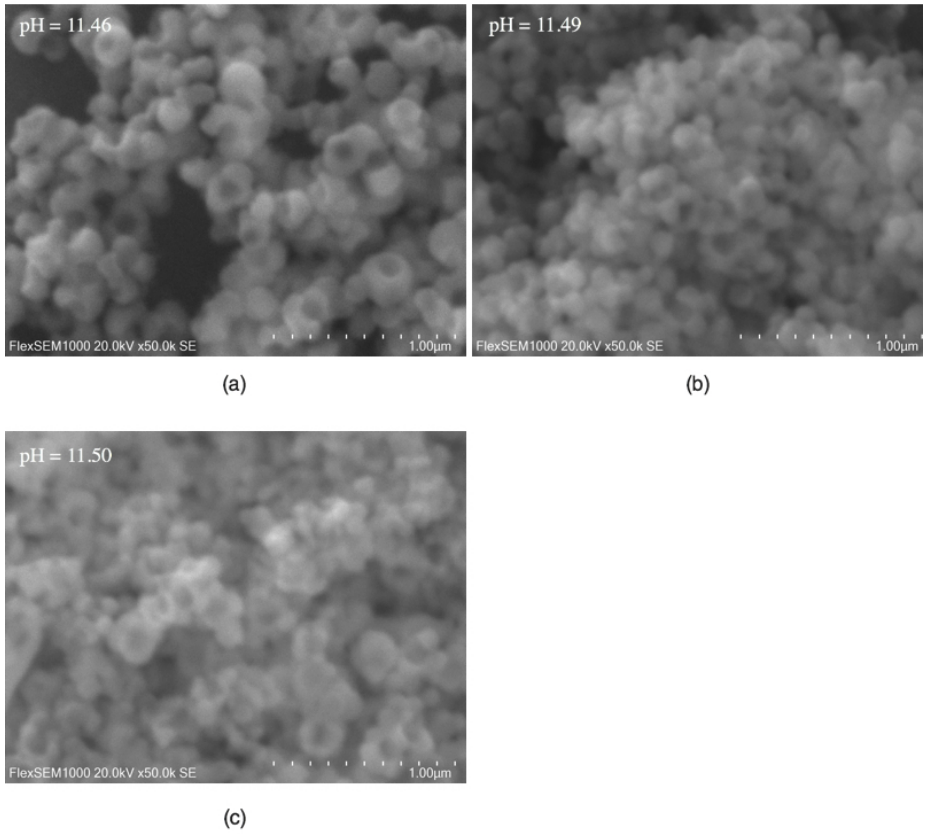

Figure C.8: SEM micrographs of the functionalised HSNS samples, HSNSfP(160)11.461 (a), HSNSfP(160)11.491 (b) and HSNSfP(160)11.502 (c).

FTIR spectra

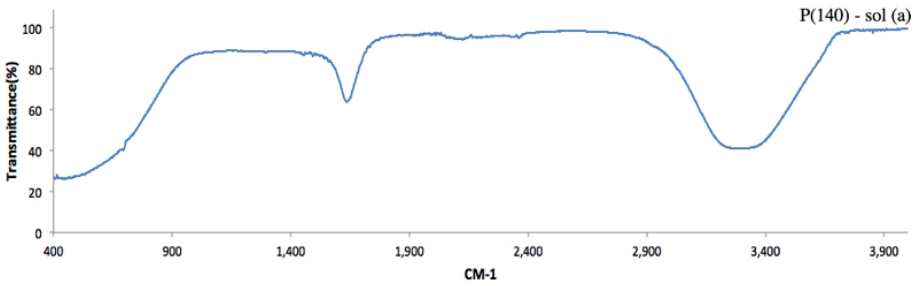

Figure C.9: FTIR spectra of the polystyrene batch P(140) in a solution (a) containing contaminants such as water. This solution of polystyrene are used for further preparation of HSNS.

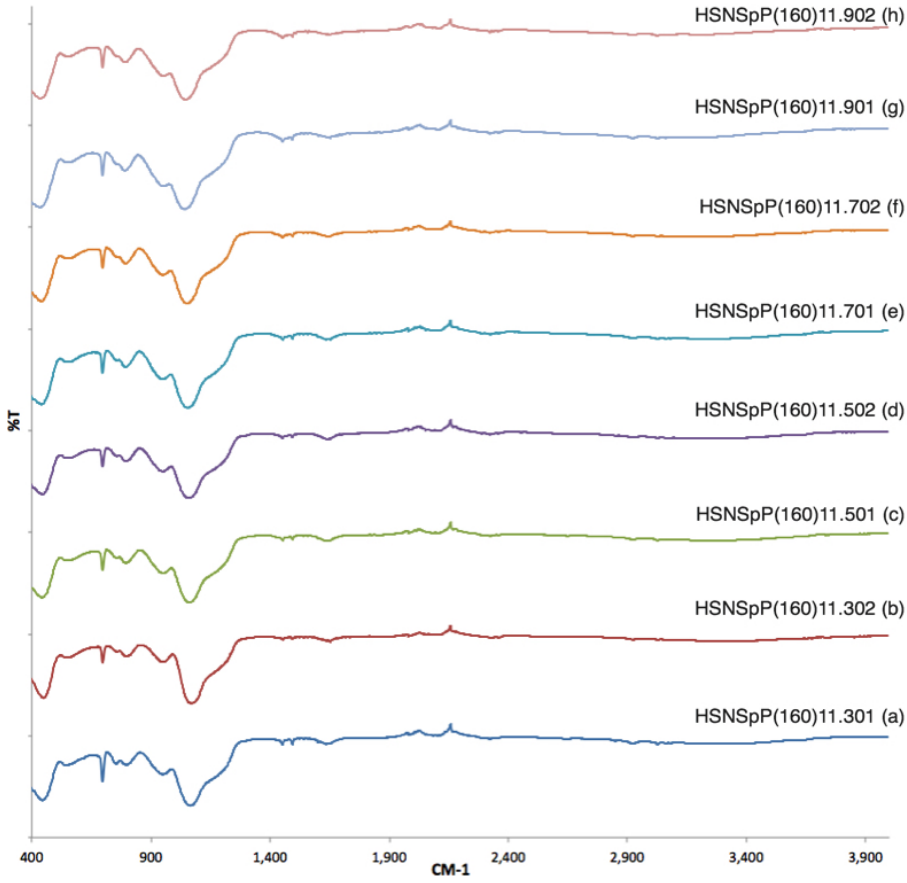

Figure C.10: FTIR spectra of eight silica coated polystyrene samples in a order based on the coating pH (low to high).

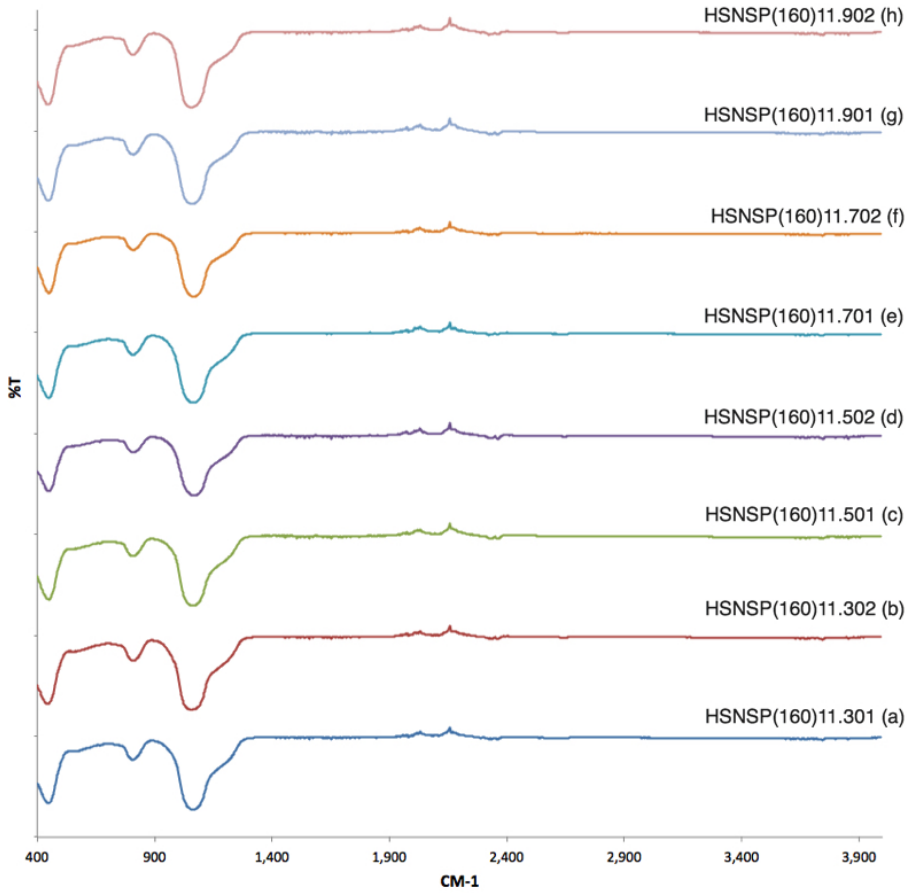

Figure C.11: FTIR spectra of eight as - synthesised HSNS samples in a order based on the coating pH (low to high).

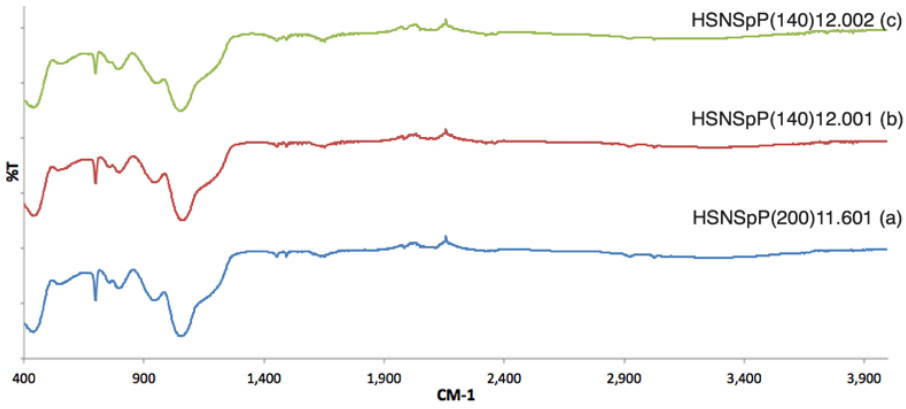

Figure C.12: FTIR spectra of three silica coated polystyrene samples in a order based on the coating pH (low to high).

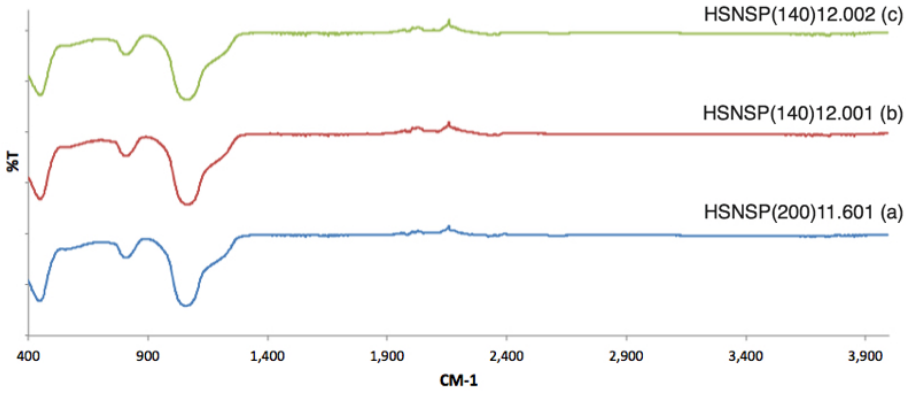

Figure C.13: FTIR spectra of three as - synthesised HSNS samples in a order based on the coating pH (low to high).

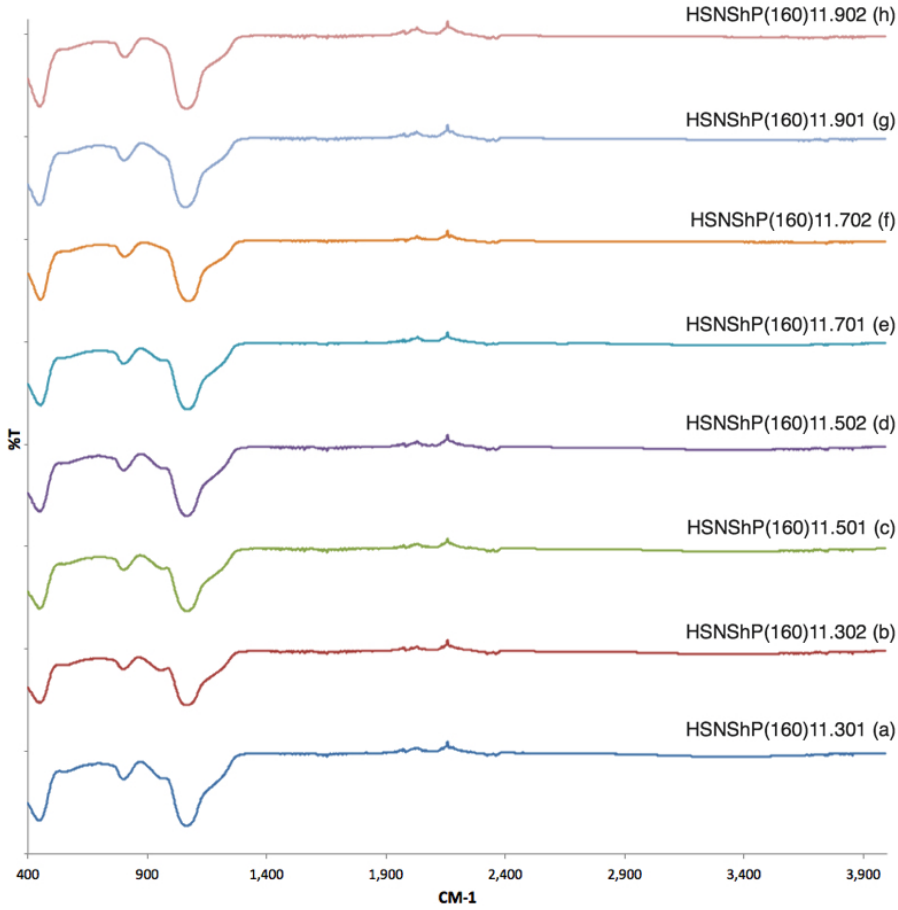

Figure C.14: FTIR spectra of eight hydroxylated HSNS samples in a order based on the coating pH (low to high).

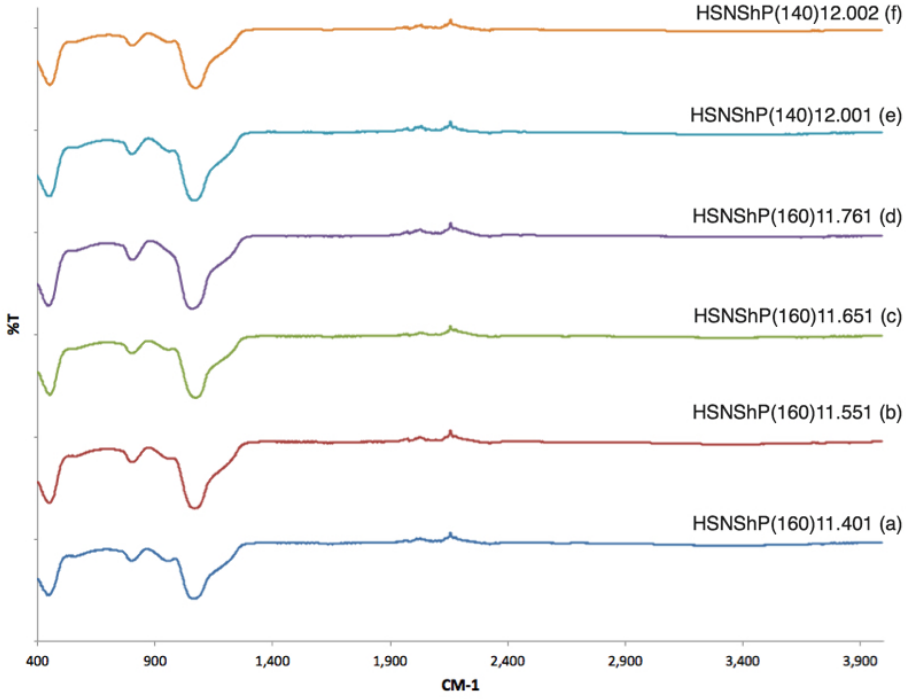

Figure C.15: FTIR spectra of six hydroxylated HSNS samples in a order based on the coating pH (low to high).

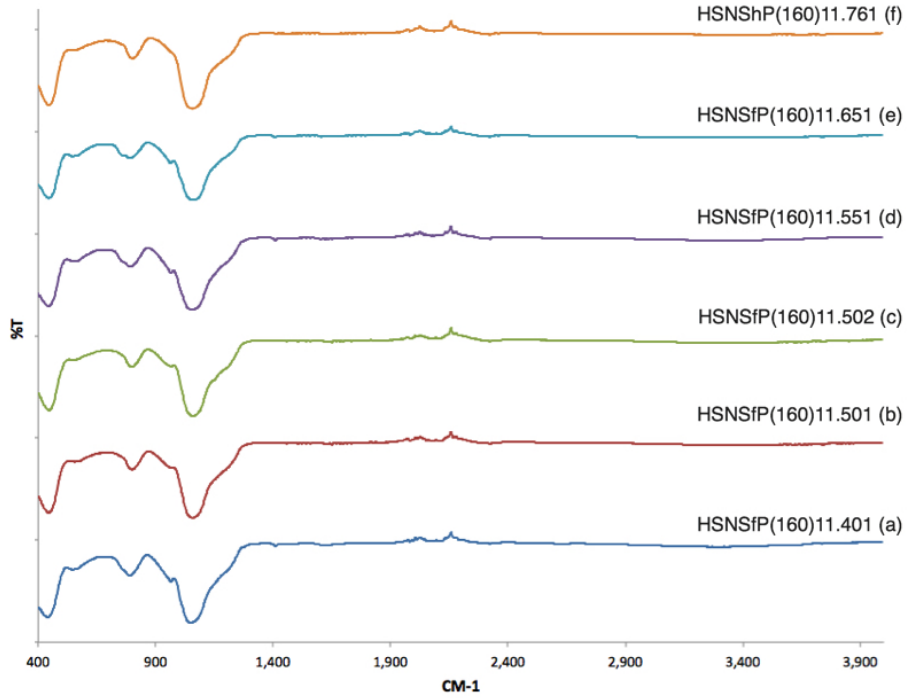

Figure C.16: FTIR spectra of six functionalised HSNS samples in a order based on the coating pH (low to high).

Thermal conductivity (Hot disk)

Sample:	Th.Conductivity (WmK^{-1})	Disk Res. (Ω)
HSNSfP(160)11.461 (1)	0.06425	12.4256
HSNSfP(160)11.461 (2)	0.06407	12.4251
HSNSfP(160)11.461 (3)	0.06408	12.4273
HSNSP(160)11.491 (1)	0.06544	12.4731
HSNSP(160)11.491 (2)	0.06497	12.4647
HSNSP(160)11.491 (3)	0.06497	12.4646

Table C.1: Thermal conductivity measurements and their respective disk resistances (Ω) for the functionalised HSNS sample, HSNSfP(140)11.461 and the as - synthesised HSNS sample, HSNShP(140)11.491. The thermal conductivity was tested three times for each material and the average value of these are represented in the Equations 4.2 and 4.1.

Overview (Tables)

Table C.2: Morphology, composition and hydrophobicity of 11 as - synthesised HSNS samples. In a order based on the coating pH (low to high).

No:	Sample	Silica coated polystyrene	As - synthesised
1	HSNSP(160)11.191	Formation of blocks	Severely altered (burned)
2	HSNSP(160)11.261	Formation of blocks	Severely altered (burned)
3	HSNSP(140)11.301	Formation of blocks	Severely altered (burned)
4	HSNSP(140)11.301	Formation of blocks	Severely altered (burned)
5	HSNSP(160)11.303	Porous, 50 nm coating (SEM) Polystyrene and SiO2 identified (FTIR)	Structure intact (SEM) SiO2 identified (FTIR) Hydrophilic
6	HSNSP(160)11.304	Unsuccessful (External heat source promoted evaporation)	-
7	HSNSP(160)11.401	Porous, 40 nm coating (SEM) Polystyrene and SiO2 identified (FTIR)	Structure intact (SEM) SiO2 identified (FTIR) Hydrophilic
8	HSNSP(160)11.461	Film, 30 nm coating (SEM) Polystyrene and SiO2 identified	Structure intact (SEM) SiO2 identified (FTIR) Hydrophilic
9	HSNSP(160)11.491	Film, 35 nm coating (SEM) Polystyrene and SiO2 identified	Structure intact (SEM) SiO2 identified (FTIR) Hydrophilic
10	HSNSP(160)11.501	Porous, 40 nm coating (SEM) Polystyrene and SiO2 identified (FTIR)	Structure intact (SEM) SiO2 identified (FTIR) Polystyrene removed (TGA) Hydrophilic
11	HSNSP(140)11.521	Film, 40 nm coating (SEM) Polystyrene and SiO2 identified (FTIR)	Holes in the spheres (SEM) SiO2 identified (FTIR) Hydrophilic

Table C.3: Morphology, composition and hydrophobicity overview of 10 as -synthesised HSNS samples. In a order based on the coating pH (low to high).

No:	Sample	Silica coated polystyrene	As - synthesised
12	HSNSP(160)11.551	Film, 40 nm coating (SEM) Polystyrene, SiO2 identified (FTIR)	Holes in the spheres (SEM) SiO2 identified (FTIR) Hydrophilic
13	HSNSP(160)11.601	Film, 190 nm coating (SEM)	Holes in the spheres (SEM)
14	HSNSP(160)11.651	Film, slight aggregation (SEM) Polystyrene, SiO2 identified (FTIR)	Multiple holes in one sphere (SEM) SiO2 identified (FTIR) Hydrophilic
15	HSNSP(160)11.701	Film, 35 nm coating (SEM) Polystyren, SiO2 identified (FTIR)	Holes in the spheres (SEM) SiO2 identified (FTIR) Hydrophilic
16	HSNSP(160)11.721	Film, 500 nm aggregated sphere (SEM) Polystyrene, SiO2 identified (FTIR)	Multiple holes in one sphere (SEM) SiO2 identified (FTIR) Hydrophobic
17	HSNSP(160)11.761	Film, 600 nm aggregated sphere (SEM) Polystyrene, SiO2 identified (FTIR)	Multiple holes in one sphere (SEM) SiO2 identified (FTIR) Hydrophilic
18	HSNSP(160)11.901	Film, 620 nm aggregated sphere (SEM) Polystyrene, SiO2 identified (FTIR)	Multiple holes in one sphere (SEM) SiO2 identified (FTIR) Hydrophobic
19	HSNSP(160)11.902	Film, 600 nm aggregated sphere (SEM) Polystyrene, SiO2 identified (FTIR)	Multiple holes in one sphere (SEM) SiO2 identified (FTIR) Hydrophilic
20	HSNSP(140)12.001	Film, 50 nm coating (SEM) Polystyrene, SiO2 identified (FTIR)	Holes in the spheres (SEM) SiO2 identified (FTIR)
21	HSNSP(140)12.002	Film 50 nm coating (SEM) Polystyrene, SiO2 identified (FTIR)	Holes in the spheres (SEM) SiO2 identified (FTIR)

Table C.4: Morphology, composition and hydrophobicity overview of 11 hydroxylated, hydrophobisated and functionalised HSNS samples. In a order based on the coating pH (low to high)

Nr:	Hydroxylation	Hydrophobisation	Functionalisation
1	-	-	-
2	-	-	-
3	-	-	-
4	-	-	-
5	Structure Intact (SEM) OH - groups identified (FTIR) Hydrophilic	Structure intact (SEM) No component change (FTIR) Hydrophilic	Structure intact (SEM) C=C - bonds identified (FTIR) Hydrophobic
6	-	-	-
7	Structure intact (SEM) OH - groups identified (FTIR) Hydrophilic	-	Structure intact (SEM) C=C - bonds identified (FTIR) Hydrophobic (contact angle)
8	Structure intact (SEM) OH - groups identified (FTIR) Hydrophilic	-	Structure intact (SEM) C=C - bonds identified (FTIR) Hydrophobic
9	Structure intact (SEM) OH - groups identified (FTIR) Hydrophilic	-	Structure intact (SEM) C=C - bonds identified (FTIR) Hydrophobic
10	Structure intact (SEM) OH - groups identified (FTIR) Hydrophilic	Structure intact (SEM) No component change (FTIR) Hydrophilic	Structure intact (SEM) No component change (FTIR) Hydrophobic
11	Structure intact (SEM) OH - groups identified (FTIR) Hydrophilic	Structure intact (SEM) No component change (FTIR) Hydrophilic	-

Table C.5: Morphology, composition and hydrophobicity overview of 10 hydroxylated, hydrophobisated and functionalised HSNS samples. In a order based on the coating pH (low to high)

Nr:	Hydroxylation	Hydrophobisation	Functionalisation
12	Structure intact (SEM) OH-groups identified (FTIR) Hydrophilic	-	Structure intact (SEM) C=C - bonds identified (FTIR) Hydrophobic (contact angle)
13	-	-	-
14	Structure intact (SEM) OH - groups identified (FTIR) Hydrophilic	-	Structure intact (SEM) C=C - bonds identified (FTIR) Hydrophobic (contact angle)
15	Structure intact (SEM) OH- groups identified (FTIR) Hydrophilic	Structure intact (SEM) No component change (FTIR) Hydrophilic	-
16	Structure intact (SEM) Uncertain identification of OH - groups (FTIR) Hydrophobic	Structure intact (SEM) No component change (FTIR) Hydrophobic	-
17	Structure intact (SEM) Uncertain identification of OH - groups (FTIR) Hydrophobic	-	Structure intact (SEM) No component change (FTIR) Hydrophobic (contact angle)
18	Structure intact (SEM) Uncertain identification of OH - groups (FTIR) Hydrophobic	-	-
19	Structure intact (SEM) OH - groups identified (FTIR) Hydrophilic	Structure intact (SEM) No component change (FTIR) Hydrophilic	-
20	Structure intact (SEM) OH- groups identified (FTIR) Hydrophilic	Structure intact (SEM) No component change (FTIR) Hydrophilic	-
21	Structure intact (SEM) OH - groups identified (FTIR) Hydrophilic	Structure intact (SEM) No component change (FTIR) Hydrophilic	

Appendix D

Documentation

Lånekassen

Ekstrastipend for søkjarar med nedsett funksjonsevne hausten 2017 og våren 2018

Gjeld ikkje for søkjarar som tek vidaregåande opplæring med ungdomsrett

X

Nynorsk

Kven kan få ekstrastipend?
Ekstrastipend kan bli gitt i tillegg til vanleg utdanningsstøtte og er på 3 631 kroner per månad. Stipendet er meint for søkjarar som er i stand til å studere, men som på grunn av nedsett funksjonsevne bruker så mykje tid og krefter på å studere, at dei ikkje kan ha lønna arbeid ved sidan av utdanninga utan at det går ut over normal studieprogresjon. Det er lege, spesialist eller annan fagperson med særleg kjennskap til den nedsette funksjonsevna som må gjere ei vurdering/utgreiing av funksjonsevna til søkjaren. For at søkjaren skal ha rett til ekstrastipend, må legen stadfeste at søkjaren, på grunn av nedsett funksjonsevne, bruker vesentleg meir tid og krefter i løpet av dagen enn andre studentar på same studium. For eksempel må søkjaren bruke betydeleg meir ressursar på å lese pensum, eller søkjaren må, på grunn av bevegelsesvanskar, bruke vesentleg meir tid og krefter på å komme seg til og frå lærestaden.

Søknadsfrist
Du må sende skjemaet i posten. Det må ha komme inn til Lånekassen innan 15. november 2017 for hausten og 15. mars 2018 for våren.

Hugs å søkje om støtte
Dersom du ikkje allereie har søkt, må du hugse å sende inn søknad om stipend og lån på www.lanekassen.no for same periode som du skal søkje om ekstrastipend for. Søknadsfristane er dei same som for ekstrastipendet.

Ekstra støtte til sommaren og stipend til forseinking
Du kan også søkje om
- stipend og lån for sommaren. Bruk skjema Y, som du kan skrive ut frå www.lanekassen.no/skjema_nn
- stipend til forseinking utover eitt undervisningsår / 60 studiepoeng

Les meir på www.lanekassen.no/nedsettfunksjonsevne.

1 Personlege opplysningar

Kundenummer i Lånekassen	Fødselsnummer (11 siffer)
2477688	30049347967
Etternamn	**Fornamn og mellomnamn**
SOLIBAKKE	PER
Adresse	**Postnummer/-stad**
HATLAVIKA 1	6016

2 Stadfesting frå lege

Les øvst på sida om kven som kan få ekstrastipend. Pass på at punkt 1 er utfylt før du krysser av i punkt 2.
Lånekassen kan også godta stadfesting frå spesialist/fagperson med særskilt kjennskap til den nedsette funksjonsevna.

Må søkjaren på grunn av nedsett funksjonsevne bruke betydeleg meir tid og krefter på utdanninga enn det som er vanleg? Ved å svare **Ja** stadfester du at dennedsette funksjonsevna fører til at søkjaren må bruke vesentleg meir tid og krefter på å studere enn andre studentar i same utdanning, som ikkje har nedsett funksjonsevne. Du stadfester at den ekstra tidsbruken er nødvendig for at søkjaren kan opprettholde normal studieprogresjon.	☒ Ja ☐ Nei
Fører den nedsette funksjonsevna til at søkjaren ikkje kan ha lønna arbeid ved sidan av utdanninga utan at det går ut over normal studieprogresjon? Ved å svare **Ja** stadfester du at konsekvensen av at søkjaren må bruke ekstra tid på studiet, er at søkjaren ikkje har kapasitet til å ha nokon form for lønna arbeid ved sidan av studiet i den perioden stadfestinga gjeld for. Merk: Søkjaren kan ikkje ha arbeid i det heile teke så lenge han/ho får dette stipendet. Det gjeld for	☒ Ja ☐ Nei

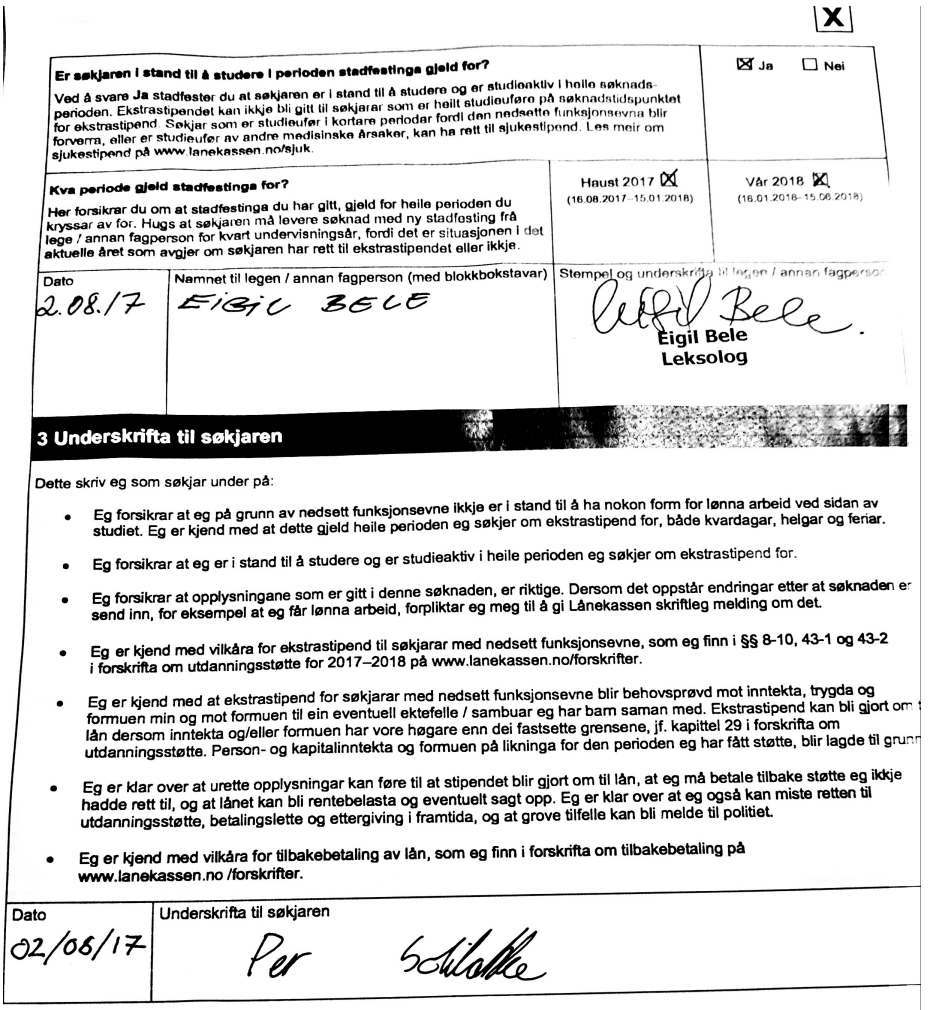

X

Er søkjaren i stand til å studere i perioden stadfestinga gjeld for?

Ved å svare **Ja** stadfester du at søkjaren er i stand til å studere og er studieaktiv i heile søknadsperioden. Ekstrastipendet kan ikkje bli gitt til søkjarar som er heilt studieuføre på søknadstidspunktet for ekstrastipend. Søkjar som er studieuføre i kortare periodar fordi den nedsette funksjonsevna blir forverra, eller er studieuføre av andre medisinske årsaker, kan ha rett til sjukestipend. Les meir om sjukestipend på www.lanekassen.no/sjuk.

☒ Ja ☐ Nei

Kva periode gjeld stadfestinga for?

Her forsikrar du om at stadfestinga du har gitt, gjeld for heile perioden du kryssar av for. Hugs at søkjaren må levere søknad med ny stadfesting frå lege / annan fagperson for kvart undervisningsår, fordi det er situasjonen i det aktuelle året som avgjer om søkjaren har rett til ekstrastipendet eller ikkje.

Haust 2017 ☒ (16.08.2017–15.01.2018)

Vår 2018 ☒ (16.01.2018–15.06.2018)

Dato	Namnet til legen / annan fagperson (med blokkbokstavar)	Stempel og underskrift til legen / annan fagperson
2.08.17	EIGIL BELE	Eigil Bele Leksolog

3 Underskrifta til søkjaren

Dette skriv eg som søkjar under på:

- Eg forsikrar at eg på grunn av nedsett funksjonsevne ikkje er i stand til å ha nokon form for lønna arbeid ved sidan av studiet. Eg er kjend med at dette gjeld heile perioden eg søkjer om ekstrastipend for, både kvardagar, helgar og feriar.
- Eg forsikrar at eg er i stand til å studere og er studieaktiv i heile perioden eg søkjer om ekstrastipend for.
- Eg forsikrar at opplysningane som er gitt i denne søknaden, er riktige. Dersom det oppstår endringar etter at søknaden er send inn, for eksempel at eg får lønna arbeid, forpliktar eg meg til å gi Lånekassen skriftleg melding om det.
- Eg er kjend med vilkåra for ekstrastipend til søkjarar med nedsett funksjonsevne, som eg finn i §§ 8-10, 43-1 og 43-2 i forskrifta om utdanningsstøtte for 2017–2018 på www.lanekassen.no/forskrifter.
- Eg er kjend med at ekstrastipend for søkjarar med nedsett funksjonsevne blir behovsprøvd mot inntekta, trygda og formuen min og mot formuen til ein eventuell ektefelle / sambuar eg har barn saman med. Ekstrastipend kan bli gjort om t lån dersom inntekta og/eller formuen har vore høgare enn dei fastsette grensene, jf. kapittel 29 i forskrifta om utdanningsstøtte. Person- og kapitalinntekta og formuen på likninga for den perioden eg har fått støtte, blir lagde til grunn
- Eg er klar over at urette opplysningar kan føre til at stipendet blir gjort om til lån, at eg må betale tilbake støtte eg ikkje hadde rett til, og at lånet kan bli rentebelasta og eventuelt sagt opp. Eg er klar over at eg også kan miste retten til utdanningsstøtte, betalingslette og ettergiving i framtida, og at grove tilfelle kan bli melde til politiet.
- Eg er kjend med vilkåra for tilbakebetaling av lån, som eg finn i forskrifta om tilbakebetaling på www.lanekassen.no /forskrifter.

Dato	Underskrifta til søkjaren
02/08/17	Per Schalke

Skjemaet sender du til Lånekassen, Postboks 4551, 8608 Mo i Rana.
Les meir på www.lanekassen.no/nedsettfunksjonsevne.

Skjema X – nynorsk – 06.2017 – side 2 av 2

Figure D.2: Documentation for dyslexia, page two.